Igneous petrogenesis of magnesian metavolcanic rocks from the central Klamath Mountains, northern California

W. G. ERNST, B. R. HACKER — *Department of Geology, School of Earth Sciences, Stanford University, Stanford, California 94305-2115*
M. D. BARTON — *Department of Earth and Space Sciences, University of California, Los Angeles, California 90024-1567*
GAUTAM SEN — *Department of Geology, Florida International University, Miami, Florida 33199*

ABSTRACT

Mafic meta-igneous supracrustal rocks in the east-central part of the western Triassic and Paleozoic belt are interlayered with and appear to predominantly overlie fine-grained clastic and cherty metasedimentary strata. This complex constitutes a lithostratigraphic terrane exposed in the vicinity of Sawyers Bar, California. Basaltic flows, dikes, and sills are informally referred to as the "Yellow Dog greenstones." Dark-colored, amygdaloidal flow breccias rich in titanium, iron, phosphorus, and light rare-earth elements (LREE's) constitute the lowest, mildly alkalic members of the mafic flow series, intimately interlayered with fine-grained terrigenous detritus. Element proportions suggest that the dark, Ti + Fe* + P-rich basaltic lavas may have been extruded in an oceanic intraplate setting. Interstratification with distal turbiditic strata indicates concurrent submarine volcanism and deep-sea sedimentary deposition. The main mass of the stratigraphically higher extrusive sequence is a light-colored, massive tholeiite series, poorer in Ti + Fe* + P + LREE's. Hypabyssal rocks belong exclusively to this second igneous suite. Compositions of the pale-colored, overlying basaltic/diabasic mass of the Yellow Dog greenstone section are consistent with eruption in an immature magmatic arc. Dikes presumably comagmatic with terminal-stage Yellow Dog volcanism cut the overlying, more eastern Stuart Fork terrane.

The Yellow Dog greenstones contain relict magmatic clinopyroxene and/or pargasitic hornblende. Both melt series include Mg-rich units (ave$_{17}$: MgO = 14.4 ± 1.9 wt. %; Cr = 650 ± 200 ppm; Ni = 270 ± 100 ppm). Sea-floor alteration apparently affected these mafic rocks in the marine environment following eruption, as reflected by $\delta^{18}O$, MgO, and CaO/Al_2O_3 values and by minor alkali and silica metasomatism. Yellow Dog igneous activity was extinguished during mid-Jurassic suturing of the oceanward Sawyers Bar terrane against and beneath the pre-existing landward Stuart Fork blueschist complex of Late Triassic metamorphic age. Subsequently, the terrane amalgam was invaded by Middle/Late Jurassic granitoids. Minor chemical alteration, including ^{18}O enrichment, also probably accompanied later regional, and especially contact, metamorphism. Nevertheless, many major-, minor-, and rare-earth-element variations in the Yellow Dog greenstones are compatible with igneous fractional crystallization trends but exclude the assimilation of significant amounts of sialic crust.

INTRODUCTION

The Klamath Mountains consist of five fault-bounded, east-dipping composite terranes (Irwin, 1960, 1972; Davis, 1968; Burchfiel and Davis, 1981). From east to west, these are the eastern Klamath plate, the central metamorphic belt, the Stuart Fork complex, the western Triassic and Paleozoic (WTrPz) belt, and the western Jurassic belt. These terranes have been juxtaposed through inferred east-descending subduction during mid-Paleozoic to mid-Mesozoic time (Mankinen and others, 1989). The Klamaths have been intruded by Middle and Late Jurassic calc-alkaline plutons (Lanphere and others, 1968; Wright, 1982; Wright and Fahan, 1988; Irwin, 1985). The effects of at least six areally and temporally distinct metamorphic episodes, spanning the interval Middle Ordovician–Late Jurassic time, are contained in rocks of the Klamath province (Mortimer, 1985; Cotkin and Armstrong, 1987; Coleman and others, 1988).

The Stuart Fork complex consists of interleaved, chiefly blueschist-facies metacherty, metaclastic, and metamafic units that lie east of the WTrPz belt (Hotz, 1973; Borns, 1984). K/Ar and $^{40}Ar/^{39}Ar$ geochronologic data indicate that the blueschists were produced during subduction about 220+ m.y. ago (Hotz and others, 1977). The Stuart Fork complex subsequently was thrust westward over the WTrPz belt (Goodge, 1989a, 1989b); greenschist/amphibolite-facies metamorphism ascribed to this tectonic juxtaposition has been called the "Siskiyou event" by Coleman and others (1988). Rocks of the Stuart Fork and more western WTrPz belts have been overprinted by Late Jurassic–earliest Cretaceous greenschist-facies recrystallization accompanying invasion by the Middle/Late Jurassic granitoids (Lanphere and others, 1968; Irwin, 1985).

Three lithostratigraphically distinct, north-south–trending segments of the structurally lower WTrPz belt were distinguished by Irwin (1972). From east to west, these are (1) the ophiolitic North Fork terrane; (2) the Hayfork composite terrane, consisting of an older, eastern terrigenous mélange and a younger, western calc-alkaline arc (Wright, 1982); and (3) the ophiolitic Rattlesnake Creek terrane. All three units contain chert, dismembered oceanic crust, and variably disrupted volcanogenic sediments. Each contains exotic limestone blocks with late Paleozoic and Triassic fossils. Early Jurassic radiolaria occur in siliceous sediments from the North Fork, western Hayfork, and Rattlesnake Creek terranes (Irwin and others, 1978; Irwin, 1981); the eastern Hayfork contains microfossils at least as young as Late Triassic in age. Most of the central WTrPz belt has been metamorphosed to upper greenschist-facies assemblages (Hill, 1985; Mortimer, 1985; Coleman and others, 1988; Donato, 1989). Grade decreases southward from amphibolite facies in the structurally deepest parts framing the Condrey Mountain dome to prehnite-actinolite facies in the southern reaches of the Sawyers Bar area. Calc-alkaline stocks intrusive into the WTrPz

Geological Society of America Bulletin, v. 103, p. 56–72, 17 figs., 5 tables, January 1991.

account in part for the apparently komatiitic bulk-rock chemistry of the metavolcanic rocks.

GEOLOGY OF THE SAWYERS BAR AREA

The spatial dispositions of the WTrPz terranes defined by Irwin (1972) in the feebly recrystallized southern Klamath Mountains are not easily recognized in the more intensely metamorphosed northern part of the range. The geology of a part of the central WTrPz belt containing the town of Sawyers Bar, California, is presented in Figure 2. The amphibolite-grade Marble Mountain mélange, lying north of the mapped area, has age and lithologic characteristics similar to those of weakly recrystallized protoliths of the Rattlesnake Creek terrane and has been correlated with it (Donato and others, 1982; Donato, 1987; Mortimer, 1985; Coleman and others, 1988). The Marble Mountain section underlies but apparently interfingers with metaclastic and metavolcanic units that pass southward into the Sawyers Bar area (Donato, 1987; Ernst, 1991). The North Fork ophiolitic terrane (Ando and others, 1983) adjoins the Sawyers Bar area directly to the south; it has been described as an amalgamation of the more western Salmon River andesitic(?) terrane and the more eastern North Fork *sensu stricto* metasedimentary and ophiolitic terrane (Blake and others, 1982; Silberling and others, 1987). A single, strongly discordant U/Pb age of 245-?10 Ma for a metagabbro sample from the North Fork ophiolite was reported by Ando and others (1983).

The distinctive metamorphosed mafic igneous suite + associated coeval sedimentary strata can be traced without interruption along strike both northeast and south of the Sawyers Bar area. Ernst (1991) argued that all supracrustal, pregranitoid units of the mapped area northwest of the thrust contact with the Stuart Fork complex belong to a single terrane; rock types within the Sawyers Bar area are similar to the North Fork lithotectonic assemblage as originally defined by Irwin (1972). Because of the uncertainties of correlation, this local, interlayered metabasaltic/metadiabasic + metaclastic unit is called the "Sawyers Bar terrane" in the present report, although we tentatively regard it as a part of Irwin's North Fork belt. The area shown in Figure 2, therefore, consists chiefly of a single lithostratigraphic unit, the Sawyers Bar terrane. A small segment of the Stuart Fork thrust sheet, intruded by the Russian Peak pluton, occupies the southeast corner of the map area (Goodge, 1989b); the English Peak pluton crops out along the western margin of the studied area. Both granitoids were emplaced during Middle/Late Jurassic time (~164–159 Ma) subsequent to, or at the end of, regional dynamothermal metamorphism in the WTrPz belt (Wright and Fahan, 1988).

The major part of the region consists of massive to weakly foliated basaltic/diabasic metavolcanics and less voluminous interlayered, chiefly metaclastic schists. Primary compositional layering and vague foliation in the greenstones and more distinct layering in the metaclastics coincide in attitude, strike north-south to N30°E, and dip steeply, predominantly to the east. The greenstones are relatively massive, but rare pillows were recognized in the northeastern part of the area near locality 127M, and as float along the southern edge of the map area west from locality 428M (Fig. 2). On the basis of top indicators at 127M, the upright synformal fold in the eastern part of the Sawyers Bar area, and stratigraphic coherence displayed by the mapped lithologies, the region is interpreted as consisting of a major greenstone synform on the east and, progressively westward, overturned, west-verging metasediment-cored antiforms and greenstone-cored synforms. Regional WTrPz belt relationships in general support this interpretation (Fig. 1). Tectonic discontinuities between metasedimentary and metavolcanic lithologic units were not recognized, although a few small lenses of serpentinite, possibly emplaced along unmapped faults, are present in the northern part of the mapped area, and larger, extensively serpentinized ultramafic bodies occur near the southwest corner of the area shown in Figure 2. Protoliths for the metasedimentary rocks consist of pelitic units, argillites, micrograywackes, calcareous quartzofeldspathics, rare limy lenses, and minor cherty horizons. Primary compositional layering in the metasediments parallels the interfingered depositional contacts with the Yellow Dog meta-extrusives.

The metavolcanics appear to be interstratified with and predominantly overlie the fine-grained metaclastics. Depositional interlayering and tight folding are evident from the intricately interdigitated outcrop patterns of the metasedimentary and mafic meta-igneous units (Fig. 2). The greenstones consist chiefly of massive flows; however, crosscutting and concordant tabular bodies, most of which display coarser-grained, relict diabasic texture, attest to the presence of hypabyssal metamorphosed mafic intrusives and slowly cooled flows within the volcanic pile and metasedimentary section. A few seemingly petrographically similar metadikes cut the Stuart Fork complex. The entire mafic meta-igneous assemblage, including associated dikes and sills, is referred to informally as the "Yellow Dog greenstones," after the prominent peak northeast of Sawyers Bar. Two compositionally distinct rock types are found in the Yellow Dog greenstones: rather schistose, dark green amygdaloidal flow breccias and more massive, light green flows + hypabyssal intrusions. Most of the former appear to be parts of a single meta-extrusive sequence interstratified with metasedimentary rocks; according to the structural interpretation, these flows underlie the main mass of lighter-colored Yellow Dog greenstones. Other, smaller, less continuous lenses of the darker, schistose metavolcanic unit are distributed within the main belt of metabasalts (Fig. 2). Most of the massive, relatively light-colored greenstones and intrusive equivalents are pale apple-green or light gray. Both darker and lighter types are, in fact, basaltic in composition, as indicated by petrographic and bulk-rock chemical data, but the dark green lithologies are enriched in Fe^{*} + Ti as well as P, Hf, Zr, Ta, La, Ce, Nd, Sm, and Eu compared with the lighter meta-igneous rocks.

Metamorphic recrystallization under physical conditions of the upper greenschist to prehnite-actinolite facies (Donato and others, 1982; Mortimer, 1985; Coleman and others, 1988; B. R. Hacker and others, unpub. data) has obliterated most original minerals and textures in the rather massive meta-igneous units. Subophitic/diabasic textures and rare relict clinopyroxene or more abundant magmatic hornblende ± zoned calcic plagioclase ± spinel ± apatite, however, have been preserved in some of the coarser-grained, principally hypabyssal rocks, amygdules, breccia clasts, and pillows in a few of the flows, and lapilli(?) in several metatuffs. Metasedimentary strata preserve compositional layering thought to represent original bedding, but top indicators are lacking. Biotite is an important phase in metasedimentary (especially pelitic and quartzofeldspathic) units and is a widespread accessory in the metavolcanics. The typical regional metamorphic assemblage of the latter is albite + chlorite + actinolitic hornblende + epidote + sphene ± minor white mica, K-feldspar, and/or quartz. Judging from experimental P-T location of the greenschist–epidote amphibolite–facies boundary (Liou and others, 1974; Apted and Liou, 1983), and occurrences of andalusite in metasedimentary rocks directly north of the mapped area (Donato, 1987), Ernst (1987) estimated P-T conditions for greenschist-facies metamorphism at Sawyers Bar as about 400 ± 75 °C, 3 ± 1 kbar.

Country rocks of the studied area are transected by at least two distinctly different kinds of dike in addition to granodioritic plutons and related finer-grained dioritic apophyses. (1) Small numbers of rhyolite-porphyry dikes crop out throughout the area, lack magmatic clinopyroxene + hornblende, and are peculiar in the ubiquitous occurrence of large books of primary muscovite ± minor garnet. Although deuterically altered, the felsite dikes are not foliated and retain igneous textures. They appear to have been injected after the regional metamorphism of the Sawyers Bar terrane and, judging from their peraluminous compositions, probably are not related to Middle/Late Jurassic calc-alkaline plutons in the area. (2) Throughout the mapped region and west at least as far as adja-

and adjacent belts to the east are as old as 165–170 Ma (U-Pb and K-Ar radiometric ages presented by Lanphere and others, 1968; Wright, 1982; Snoke and others, 1982; Irwin, 1985; Wright and Fahan, 1988). Accordingly, the WTrPz belt must have been accreted to the more eastern Klamath lithotectonic entities and been regionally metamorphosed by mid-Jurassic time.

The present study focuses on the igneous petrogenesis of a metabasaltic series that contains unusually magnesian, komatiitic(?) metavolcanics located near Sawyers Bar, California (Ernst, 1987), along and west of the east-dipping thrust contact juxtaposing structurally higher Stuart Fork and underlying WTrPz belt lithologies. Regional geologic/tectonic relations in the central Klamaths and the location of the study area are shown in Figure 1. A possible companion paper describing the polymetamorphism of these greenstones concludes that although many of their bulk-rock major- and trace-element contents are relatively undisturbed, minor to significant changes occurred in alkali, lime, magnesia, and oxygen isotope concentrations in most samples. Metasomatic increases in MgO and CaO relative to Al_2O_3 appear to be large enough to

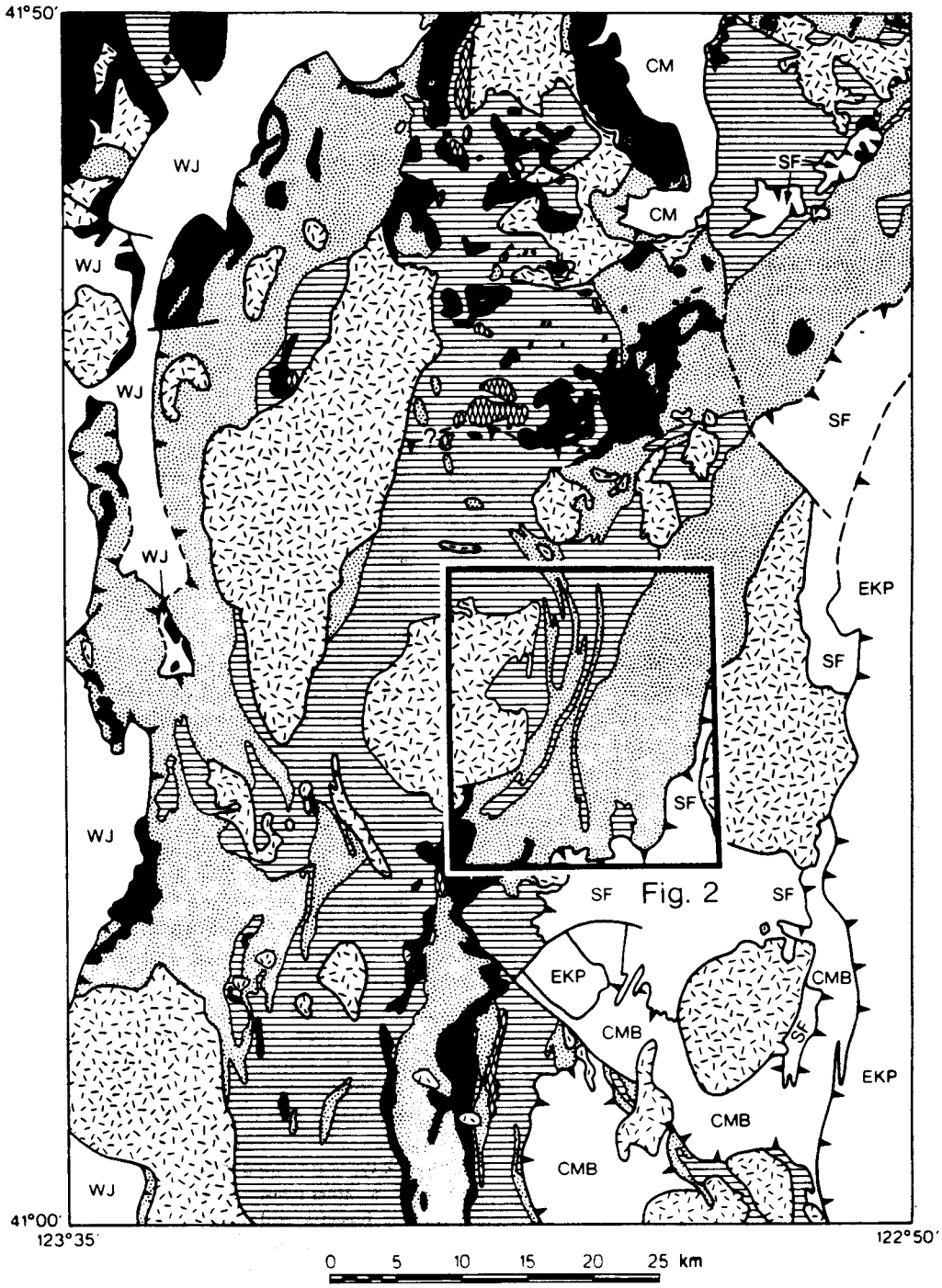

Figure 1. Regional lithotectonic units of the western Triassic and Paleozoic (WTrPz) belt of the central Klamath Mountains, after Wagner and Saucedo (1987) and Ernst (1991). Units are as follows: black, serpentinized peridotites; random dashes, Jurassic/Cretaceous granitoid intrusions; stippled pattern, mafic metavolcanics; horizontal lines, metasedimentary strata; cross-hatch pattern, marble beds and blocks. Abbreviations are EKP, eastern Klamath plate; CMB, central metamorphic belt; CM, Condrey Mountain terrane; SF, Stuart Fork complex; WJ, western Jurassic belt. Barbs are shown on upper plates of thrust sheets. Location of the Sawyers Bar map area is indicated as Figure 2.

TABLE 1. ESTIMATED AVERAGE PETROGRAPHIC MODES OF YELLOW DOG META-IGNEOUS ROCK TYPES, SAWYERS BAR TERRANE (vol. %)

Mineral	Rock type (no. of samples)			
	Serpentinite (18)	Darker volcanic (30)	Lighter volcanic (72)	Lighter hypabyssal (81)
Quartz	—	2	2	4
Albite	—	18	29	40*
Clinopyroxene	3†	tr†	2†	7†
Orthopyroxene	1†	—	—	—
Olivine	3†	—	—	—
Amphibole	17	40	32*	27*
Biotite	—	2	1	1
White mica	—	1	1	1
Chlorite	2	17	10	8
Talc	16	—	—	tr
Serpentine	51	—	—	—
Epidote-clinozoisite	—	10§	15§	8§
Carbonate	2	2	3	1
Opaques/ores	5	4	2	1
Sphene	—	4	3	2

*Includes relict igneous cores; † relict igneous phase; § minor prehnite ± stilbite ± pumpellyite.

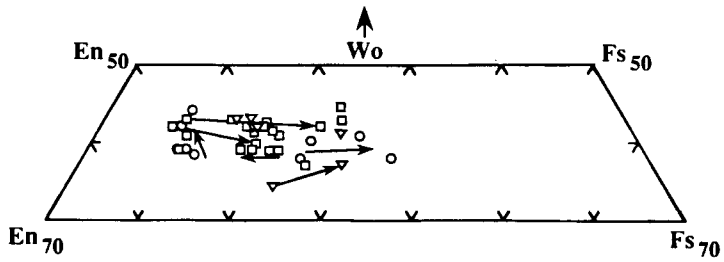

Figure 3. Yellow Dog relict igneous clinopyroxenes. Sample symbols as in Figure 2. Arrows indicate core-to-rim variation for individual samples.

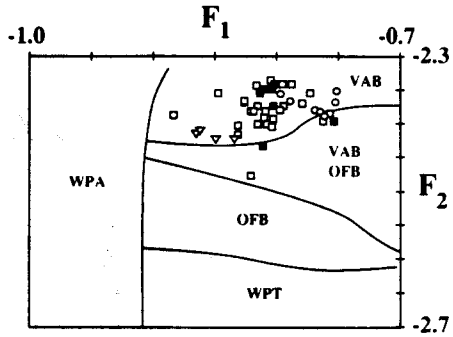

Figure 4. Plot of discriminant functions F_1 versus F_2 for Yellow Dog relict igneous clinopyroxenes, after Nisbet and Pearce (1977). Sample symbols as in Figure 2. VAB, volcanic-arc basalt; OFB, ocean-floor basalt; WPT, within-plate tholeiite; WPA, within-plate alkali basalt. $F_1 = -0.012\ SiO_2 - 0.0807\ TiO_2 + 0.0026\ Al_2O_3 - 0.0012\ FeO^* - 0.0026\ MnO + 0.0087\ MgO - 0.0128\ CaO - 0.0419\ Na_2O$. $F_2 = -0.0469\ SiO_2 - 0.0818\ TiO_2 - 0.0212\ Al_2O_3 - 0.0041\ FeO^* - 0.1435\ MnO - 0.0029\ MgO + 0.0085\ CaO + 0.0160\ Na_2O$. All but four compositions fall within the "VAB only" field, and those other four fall within the "VAB or OFB" field. This technique is ~70% likely to identify the correct magma type, according to Nisbet and Pearce.

morphic parageneses. Evidently Yellow Dog basaltic volcanism locally was active immediately prior to and during tectonic juxtaposition of the Sawyers Bar terrane beneath the Stuart Fork complex and over the Marble Mountain terrane.

Thrusting was accompanied and followed by pervasive, laterally gradational recrystallization of Stuart Fork, Sawyers Bar, and Marble Mountain terranes. The regional foliation is crudely parallel to the east-dipping tectonic junction of the Sawyers Bar terrane against the Stuart Fork complex and is cut by the Russian and English Peak intrusives. Regional metamorphism preceded the development of contact aureoles surrounding the Middle/Late Jurassic granodioritic plutons; this is demonstrated by hornblende overgrowths on actinolite in thermally upgraded greenschist-facies rocks and by hornfelsic overprint on the regional north-northeast–striking foliation.

PETROGRAPHY OF THE YELLOW DOG GREENSTONES

More than 300 mafic/ultramafic rock samples were collected and examined microscopically in this investigation. Average, visually estimated modes for Yellow Dog specimens are presented in Table 1. The darker, Fe^* + Ti–rich, schistose metabasalts contain greater proportions of neoblastic amphibole, chlorite, sphene, and opaque phases, compared to the epidote-rich, lighter green, more massive metabasalts and the plagioclase-rich, relict igneous hornblende- and/or clinopyroxene-bearing metadiabases. Relict cumulate textures involving olivine, pyroxenes, and/or plagioclase have not been observed in the greenstones. Fine grain size and complex textures of the rocks hampered petrographic analysis. Consequently, emphasis was placed on differentiating between igneous and metamorphic minerals by back-scattered electron microscopy and electron-probe microanalysis.

The best-preserved magmatic textures are subophitic to diabasic, with plagioclase laths approximately 100 μm long embedded in larger clinopyroxene crystals. Between 0 and about 70 vol. % igneous phases are preserved, including clinopyroxene, hornblende, plagioclase, spinel, and apatite; anorthoclase, found in a few samples, may also be an igneous mineral. Spinifex textures were not observed in this study.

RELICT IGNEOUS MINERAL CHEMISTRY OF THE YELLOW DOG GREENSTONES

Chemical Data

The compositions of phases in 37 greenstone samples were determined by electron microprobe analysis. Representative data for primary igneous clinopyroxenes, hornblendes, and plagioclases are presented in Table 2. The back-scattered electron microscopy and electron microprobe analyses were conducted with a four-spectrometer Cameca Camebax electron-probe microanalyzer at the University of California, Los Angeles, using well-characterized natural and synthetic mineral standards. Spot selection was performed in back-scattered electron mode. The electron beam diameter was 2 μm at 15 kV and 10 nA. One to five counts of 20 sec for peak intensities and 10 sec for background were made for each of 10 elements. Analyses of inhomogeneous grains are presented individually. All mineral formulas were calculated following the methods of Laird and Albee (1981).

Relict Magmatic Phases

Igneous clinopyroxene (cpx) occurs in about 10% of the rocks studied (analyses are all from the lighter-colored series, chiefly the coarser-grained hypabyssals), composing as much as 35 vol. % of the rock. Individual crystals are 50–400 μm in length and are subhedral laths or

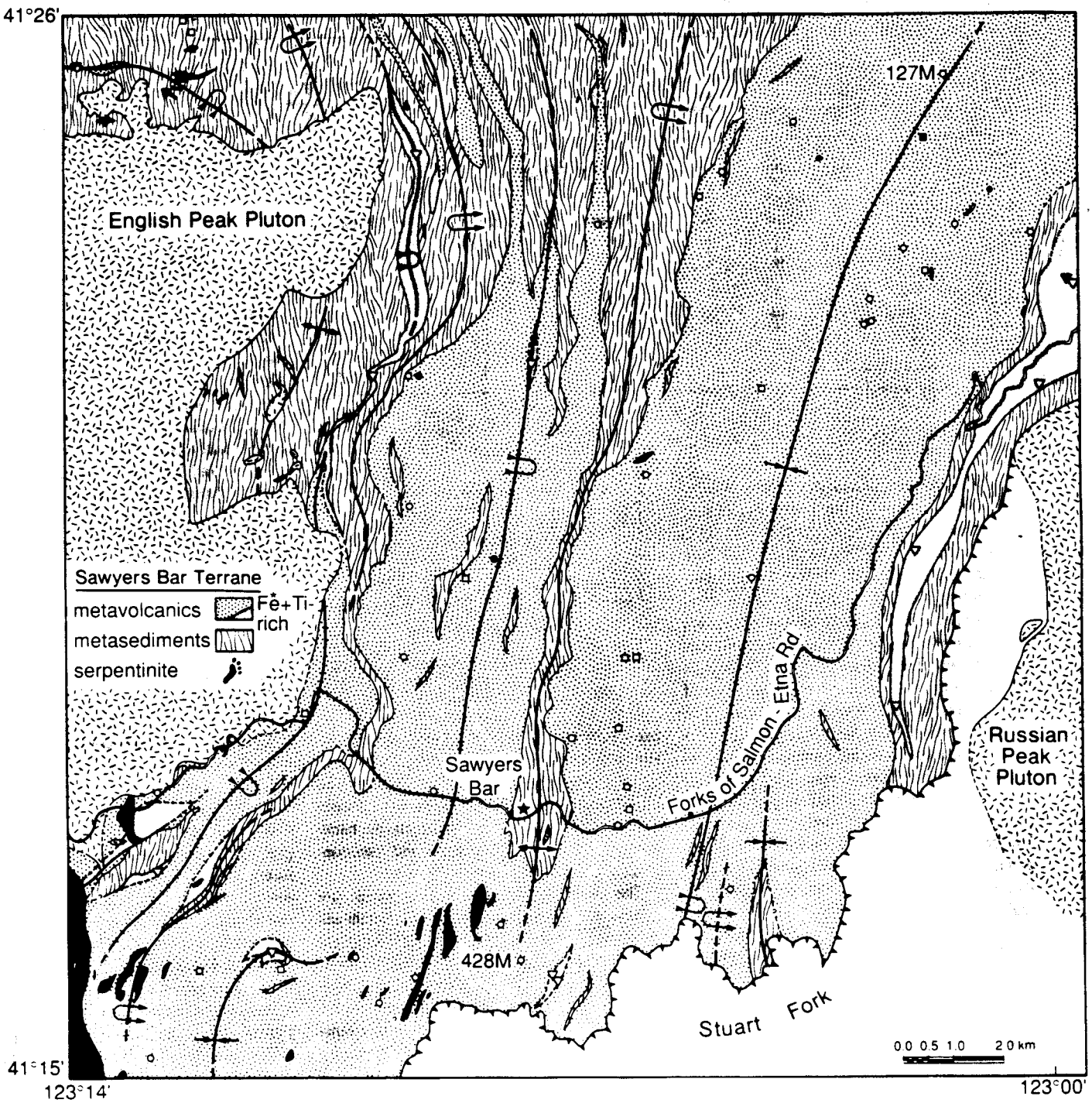

Figure 2. Geology of the Sawyers Bar area, a preliminary, areally less extensive version of which was presented by Ernst (1987). Traces of axial planes are interpretive. The town of Sawyers Bar is indicated by a black star. Sample symbols for this and most succeeding illustrations are as follows: upside-down triangles, darker, more schistose, amygdaloidal metabasalt flow breccias; circles, paler, more massive metabasalts; squares, diabasic dikes/sills; filled symbols, Mg-rich Yellow Dog meta-igneous rocks; open symbols, normal (basaltic) Yellow Dog meta-igneous rocks. Most of the region is underlain by rocks of the Sawyers Bar terrane (= North Fork terrane of Irwin, 1972); southeast of a major, east-dipping thrust fault, a small part of the Stuart Fork terrane (= Fort Jones terrane of Silberling and others, 1987) is exposed.

cent to the western margin of the English Peak pluton, clinopyroxene and/or hornblende-rich metadiabasic dikes and sills considered by us to be comagmatic with the lighter-colored Yellow Dog metabasalts intrude both Sawyers Bar and Stuart Fork terranes. Similar metahypabyssals transect Marble Mountain rocks to the north (Donato, 1985). The degree of alteration is variable among these mafic intrusives; a few are remarkably fresh and apparently unmetamorphosed, but many exhibit neoblastic overgrowths of greenschist-facies phases on relict igneous mineral cores, and the remainder are entirely transformed to metamorphic facies assemblages characteristic of the Yellow Dog metavolcanics. Complete textural/mineralogical gradations exist between the primary hypabyssal igneous assemblages and the secondary meta-

TABLE 2a. REPRESENTATIVE CHEMICAL ANALYSES OF YELLOW DOG RELICT MAGMATIC PYROXENES, SAWYERS BAR TERRANE (wt. %)

Sample	215M		221M		235M		321M		351M	
	Core	Rim	Core	Rim	Core	Rim	Core	Rim	Core	Rim
SiO_2	52.90	51.39	53.26	50.79	50.94	48.41	51.51	51.33	50.92	50.72
Al_2O_3	1.85	2.89	2.11	2.58	4.53	3.83	1.94	2.14	3.27	3.78
TiO_2	0.38	0.49	0.21	0.44	0.69	1.57	0.68	0.68	0.50	0.48
FeO*	6.75	7.48	5.53	10.23	5.77	14.04	10.98	12.15	9.37	8.57
Cr_2O_3	0.14	0.09	0.17	0.04	0.62	b.d.	0.04	b.d.	0.06	b.d.
MnO	0.13	0.24	0.18	0.27	0.19	0.40	0.32	0.36	0.29	0.23
MgO	17.70	17.23	16.82	13.97	16.84	11.46	14.94	14.18	14.16	14.79
CaO	19.37	18.52	21.19	20.03	19.79	19.66	19.25	19.13	20.56	20.71
Na_2O	0.12	0.20	0.26	0.44	0.24	0.37	0.27	0.31	0.42	0.40
Total	99.3	98.5	99.7	98.8	99.6	99.8	100.0	100.3	99.5	99.7

b.d., below detection.

image in Figure 5 documents this typically magmatic, cyclic crystallization/resorption phenomenon. Igneous amphiboles are 100–400 μm in length and are subhedral to euhedral laths and prisms. As indicated in Figure 6, they range in composition from magnesiohornblende to kaersutite and ferropargasite (Leake, 1978). Some of the igneous amphiboles are subsilicic, having as few as 5.6 Si atoms per formula unit. Igneous amphibole cores contain high A-site occupancy ($Na^A + K$), tetrahedral aluminum (Al^{IV}), and trivalent octahedral site occupancy ($Al^{VI} + Fe^{3+} + Ti$). Igneous amphibole rims contain less of all these constituents, compatible with decreasing

TABLE 2b. REPRESENTATIVE CHEMICAL ANALYSES OF YELLOW DOG RELICT MAGMATIC AMPHIBOLES, SAWYERS BAR TERRANE (wt. %)

Sample	85M	124M		212M		220M		221M		320M		321M		351M		375M	
	Core Fe-Pg	Core Ts	Rim Fe-Ts-Hb	Core Mg-Hst	Rim Mg-Hb	Core Mg-Hst	Rim Mg-Hst	Core Mg-Hst	Rim Mg-Hb	Core Mg-Hst	Rim Ts-Hb	Core Mg-Hb	Rim Mg-Hb	Core Mg-Hst	Rim Mg-Hst	Core Mg-Hst	Rim Ts-Hb
SiO_2	37.49	41.51	42.17	41.31	46.78	39.77	41.56	41.88	45.59	40.82	44.01	48.27	48.27	41.47	42.33	40.29	44.38
Al_2O_3	17.37	14.11	14.05	13.31	7.84	15.67	14.38	12.60	7.81	13.40	12.96	6.69	6.72	13.45	10.95	14.07	11.88
TiO_2	6.32	2.46	0.42	2.72	0.43	1.44	1.71	2.93	0.50	2.94	0.87	1.61	0.12	2.25	3.11	2.74	0.88
FeO*	14.86	11.11	19.08	11.38	15.59	13.24	12.80	11.76	18.04	12.25	12.29	15.80	19.20	12.18	16.59	11.97	14.05
Cr_2O_3	0.05	b.d.	0.03	b.d.	0.09	0.03	b.d.	b.d.	b.d.	0.04	0.11	0.07	b.d.	0.07	b.d.	b.d.	b.d.
MnO	0.40	0.09	0.48	0.19	0.37	0.27	0.20	0.13	0.59	0.14	0.25	0.37	0.40	0.21	0.28	0.16	0.34
MgO	7.40	13.63	6.00	14.10	14.72	11.94	12.64	13.53	10.27	13.39	13.25	12.30	9.90	13.80	10.26	12.90	11.87
CaO	10.03	11.04	10.46	11.59	11.44	11.66	11.57	11.07	10.84	11.42	11.43	11.27	11.93	11.10	10.87	11.57	11.33
Na_2O	3.04	2.12	1.98	2.19	1.16	2.42	2.22	2.35	1.87	2.26	1.75	0.99	0.72	2.66	2.29	2.21	1.96
K_2O	b.d.	0.58	0.55	0.51	0.36	0.33	0.29	0.90	0.76	0.64	0.51	0.22	0.49	0.89	1.01	1.00	0.59
Total	96.96	96.65	95.22	97.30	98.78	96.77	97.37	97.15	96.27	97.30	97.43	97.59	97.75	98.08	97.69	96.91	97.28

b.d., below detection.

TABLE 2c. REPRESENTATIVE CHEMICAL ANALYSES OF YELLOW DOG RELICT MAGMATIC PLAGIOCLASES, SAWYERS BAR TERRANE (wt. %)

Sample	57M		215M	235M		351M		354M		375M
	An_{48}	An_{49}	An_{47}	An_{50}	An_{50}	An_{38}	An_{33}	An_{42}	An_{31}	An_{29}
SiO_2	56.15	55.72	55.15	54.87	54.85	58.02	59.11	57.12	60.47	60.42
Al_2O_3	27.94	27.90	26.65	27.02	26.82	25.65	25.02	26.43	24.98	24.75
TiO_2	b.d.	b.d.	0.05	0.10	0.09	b.d.	b.d.	b.d.	0.07	b.d.
Fe_2O_3	0.31	0.18	1.05	0.99	0.92	0.18	0.07	0.23	0.12	0.20
Cr_2O_3	b.d.	b.d.	0.06	b.d.	b.d.	b.d.	0.06	0.04	0.03	0.03
MnO	b.d.	b.d.	b.d.	b.d.	0.06	0.04	b.d.	0.04	0.04	b.d.
MgO	b.d.	b.d.	0.22	0.20	0.07	b.d.	b.d.	0.12	0.04	b.d.
CaO	10.13	10.12	9.57	10.56	10.68	8.09	7.18	8.97	6.67	6.23
Na_2O	5.92	5.80	5.51	5.28	5.56	7.12	7.76	6.47	8.04	6.83
K_2O	0.07	0.07	0.62	0.32	b.d.	b.d.	b.d.	b.d.	0.10	0.08
Total	100.52	99.79	98.88	99.34	99.05	99.10	99.20	99.42	100.56	98.54

b.d., below detection

prisms. They are zoned from magnesian ($Wo_{43}En_{48}Fs_{09}$) cores to ferrous ($Wo_{37}En_{34}Fs_{29}$) rims. Clinopyroxene compositions are illustrated in Figure 3. Systematic spatial or stratigraphic variations in composition of this phase were not detected. Analyzed grains contain 0.5–4.5 wt. % Al_2O_3, $\leq$1.6 wt. % TiO_2, $\leq$0.9 wt. % Cr_2O_3, $\leq$1.2 wt. % MnO, and $\leq$0.4 wt. % Na_2O. Cpx compositions suggest that they crystallized from an arc-basalt magma (Nisbet and Pearce, 1977), as shown in Figure 4.

Relict igneous amphiboles occur in more than half of the rocks studied, in abundances as great as about 70 vol. % (Table 2). Some of these may be glomeroporphyritic in origin. Oscillatory zoning is common; the back-scattered electron

temperature during magmatic growth. Note that sample 351M contains two populations of amphiboles (Fig. 6). Magmatic amphiboles contain as much as 6.3 wt. % TiO_2, 0.4 wt. % Cr_2O_3, and 0.8 wt. % MnO.

Igneous and metamorphic plagioclase crystals are chiefly anhedral and are interstitial to amphibole and pyroxene. Identification of primary plagioclase was based on composition; relict igneous plagioclase grains are within the range An_{29-50}, whereas secondary plagioclases are albite, oligoclase (low-grade regional metamorphic), or anorthite (contact metamorphic). Fe_2O_3, MgO, K_2O, and TiO_2 compose as much as 1.1, 0.2, 0.3, and 0.1 wt. %, respectively. Two samples contain anorthoclase ($Ab_{41}An_{02}Or_{57}$ and $Ab_{14}An_{05}Or_{81}$), possibly a relict igneous phase. Some alkali feldspar crystals contain as much as 0.2–0.3 wt. % Fe_2O_3. Back-scattered electron imagery has not shown lamellae of contrasting chemistry, and so if exsolution has occurred, the alkali feldspars must be cryptoperthitic.

Relict microphenocrystic spinel in one of the Yellow Dog greenstones (diabasic sample

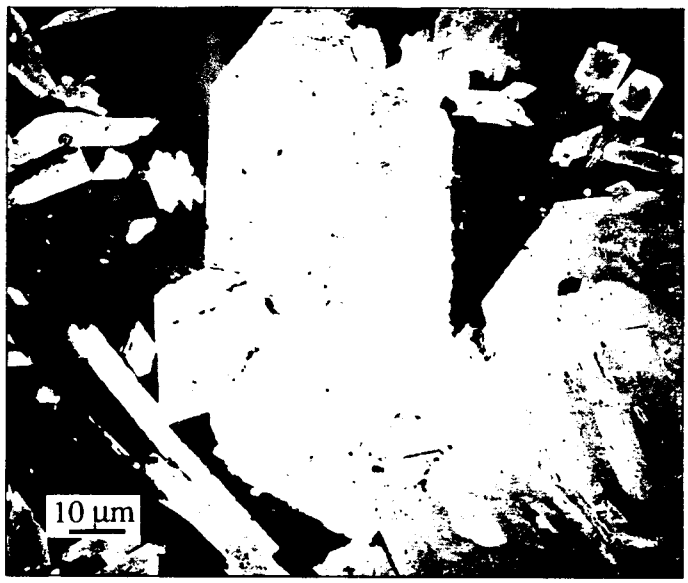

Figure 5. Back-scattered electron image of oscillatory compositional zoning in relict igneous hornblende from Yellow Dog metahypabyssal sample 249M.

212M) is magnesiochromite $(Mg_{0.6}Fe^{2+}_{0.4})(Cr_{1.3}Fe^{3+}_{0.2}Al_{0.5})O_4$, accompanying the other igneous minerals described above.

Discussion

Although some Yellow Dog greenstones are unusually Mg rich (see below), it is unlikely from a petrographic point of view that they represent komatiitic basalts. Zoned clinopyroxene is the most important phase in recognized komatiitic basalts. Although many Yellow Dog greenstones contain relict cpx, hornblende is the predominant igneous ferromagnesian mineral. The original Yellow Dog mafic volcanics contain zoned augite, whereas Archean ultramafic basalts typically contain either zoned augite or magnesian pigeonite, mantled by subcalcic augite zoned to aluminous augite (Cameron and Nisbet, 1982). Komatiitic basalts normally are inferred to have been derived from magmas that crystallized abundant olivine and pyroxene (Viljoen and others, 1982). The presence of oscillatorally zoned hornblende, clinopyroxene, and plagioclase, and the complete lack of olivine on the contrary, are compatible with crystallization of an immature arc-tholeiite magma.

BULK-ROCK CHEMISTRY OF THE YELLOW DOG GREENSTONES

Compositional Data

Greenstones in the Sawyers Bar area exhibit a systematic range of basaltic compositions, which may be ascribed to generation from chemically heterogeneous mantle protoliths or to differing degrees of partial fusion of a homogeneous ul-

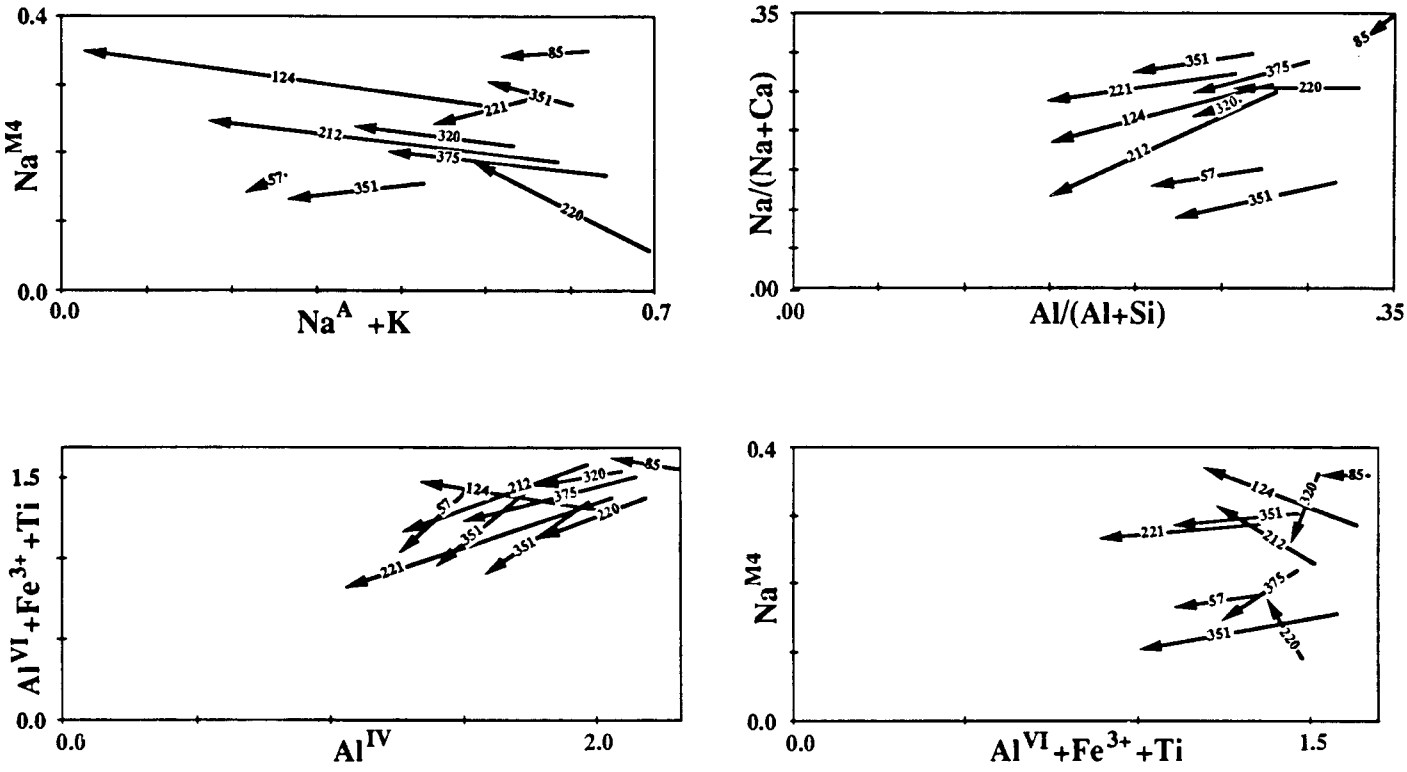

Figure 6. Compositions of Yellow Dog relict igneous amphiboles. Each arrow represents the core-to-rim compositional variation determined from at least four amphibole crystals per sample. Note that sample 351M contains two distinct populations of amphibole crystals.

TABLE 3. BULK-ROCK MAJOR- AND MINOR-ELEMENT CHEMISTRY OF YELLOW DOG METAVOLCANIC ROCKS, SAWYERS BAR TERRANE (wt. %)

	Serpentinite		Darker metavolcanics					Lighter metavolcanics					
	100M	184M	386M	424M	425M	483M	506M	391M†	428M	435M†	450M	464M	484M
SiO_2 (wt. %)	39.10	39.20	48.00	44.40	46.00	50.00	50.40	53.30	50.00	48.00	53.10	52.55	50.80
Al_2O_3	4.40	2.50	13.40	11.90	17.00	12.80	15.00	10.50	13.30	11.50	13.40	13.50	12.80
MgO	32.30	42.10	9.30	12.00	4.70	6.20	6.30	13.50	9.30	12.20	7.30	7.60	9.00
CaO	3.70	0.50	6.70	6.33	5.20	7.40	8.20	6.60	10.40	14.30	10.00	9.45	10.80
Na_2O	0.27	0.06	2.60	1.66	3.10	3.00	3.60	1.75	2.80	0.53	3.20	2.80	1.60
K_2O	0.04	0.03	0.50	0.26	2.40	0.74	0.25	1.40	0.16	1.00	0.30	0.50	0.08
Fe_2O_3*	19.30	14.80	14.90	15.00	14.30	15.00	13.70	10.00	11.10	9.60	10.70	10.80	11.50
TiO_2	0.25	0.07	2.50	2.50	3.10	2.40	1.30	0.50	0.92	0.66	0.88	0.75	0.85
MnO	0.22	0.25	0.29	0.14	0.18	0.26	0.15	0.17	0.16	0.13	0.17	0.16	0.15
P_2O_5	0.03	0.01	0.35	0.38	0.92	0.23	0.14	0.15	0.06	0.09	0.06	0.06	0.07
Loss on ignition	(8.50)	(11.37)	1.41	5.07	3.13	1.64	0.74	1.90	1.45	1.90	0.71	1.71	2.17
Total§	99.83	99.87	100.04	99.76	100.12	99.72	99.83	99.90	99.71	99.98	99.86	99.95	99.86
Cr (ppm)	1190	2283	255	361	35	101	70	630	270	420	156	310	109
Nb	—	—	20	25	20	0	20	10	0	0	20	0	0
Ni	903	1140	153	240	30	75	48	191	116	170	64	116	66
Rb	0	3	22	10	65	22	0	28	0	17	17	10	16
Sr	8	2	310	380	430	143	235	360	115	60	80	160	155
Y	—	—	25	25	25	25	0	20	17	0	16	15	0
Zr	30	15	183	190	300	118	118	144	66	65	92	79	78

	Lighter metavolcanics					Hypabyssal	Metavolcanic averages ± 1σ			
	487M	495M	516M	520bM	523M	481M	Darker (16)[a]	Lighter (38)[b]	Hypabyssal (18)[c]	Mg-rich (17)[d]
SiO_2 (wt. %)	44.70	49.50	51.00	51.40	52.80	47.60	47.88 ± 2.47	50.78 ± 1.92	53.26 ± 2.98	49.18 ± 2.52
Al_2O_3	12.70	17.40	13.30	14.00	14.80	15.30	12.86 ± 1.85	12.85 ± 1.68	14.04 ± 1.78	10.95 ± 0.99
MgO	9.60	5.90	8.30	9.00	6.70	10.60	9.95 ± 3.09	10.72 ± 2.96	9.19 ± 3.20	14.44 ± 1.91
CaO	19.50	11.50	10.10	8.90	9.00	7.80	8.44 ± 2.62	10.21 ± 2.23	8.15 ± 1.39	10.02 ± 1.99
Na_2O	0.45	3.00	2.30	3.00	1.10	2.15	2.06 ± 1.00	2.34 ± 0.77	2.43 ± 0.70	1.47 ± 0.53
K_2O	0.11	0.25	0.38	0.50	1.20	1.25	0.71 ± 0.60	0.48 ± 0.44	1.42 ± 0.62	0.77 ± 0.36
Fe_2O_3*	10.15	10.00	11.00	10.40	11.70	11.20	13.87 ± 1.20	10.73 ± 0.98	9.94 ± 1.21	11.12 ± 1.51
TiO_2	0.82	0.86	1.10	0.80	1.10	0.80	2.47 ± 0.60	0.91 ± 0.21	0.86 ± 0.17	1.16 ± 0.80
MnO	0.14	0.13	0.16	0.14	0.18	0.16	0.18 ± 0.02	0.17 ± 0.03	0.17 ± 0.02	0.17 ± 0.01
P_2O_5	0.07	0.13	0.08	0.05	0.20	0.10	0.34 ± 0.17	0.11 ± 0.05	0.22 ± 0.08	0.20 ± 0.11
Loss on ignition	2.04	1.03	2.44	1.50	1.10	2.74				
Total§	100.32	99.76	100.21	99.77	99.97	99.77				
Cr (ppm)	118	132	187	327	152	280	239 ± 176	310 ± 251	283 ± 229	649 ± 199
Nb	0	0	0	0	0	20				
Ni	72	73	80	137	30	272	159 ± 135	122 ± 96	100 ± 86	267 ± 105
Rb	0	10	10	10	44	10	15 ± 17	11 ± 11	35 ± 19	16 ± 10
Sr	115	250	129	210	510	108	382 ± 204	179 ± 102	383 ± 210	285 ± 222
Y	15	33	33	0	25	0				
Zr	65	105	78	92	118	65	193 ± 57	76 ± 27	113 ± 50	125 ± 79

†metakomatiitic(?) basalt. §Serpentinites recalculated to 100% on an anhydrous basis.
a = 1M, 11M, 38M, 89M, 91M, 153M, 170M, 201M, 207M, 354M, 372M, 386M, 424M, 425M, 483M, 506M.
b = 391M, 428M, 435M, 450M, 464M, 484M, 487M, 495M, 516M, 520bM, 523M, and all analyses from Ernst (1987, Tables 2a and 2b) except those noted in footnote a.
c = 481M and 17 analyses from Ernst (1987, Table 2c).
d = 81M, 391M, 435M, and 14 analyses from Ernst (1987, Table 6).
X-ray fluorescence analyses by G. Stummer, University of California, Los Angeles.

tramafic source. In either scenario, the product liquids may also have been subjected to variable extents of fractional crystallization and/or assimilation of crustal lithologies attending decompression and cooling on ascent into the crust. Additionally, sea-floor, regional, and contact metamorphism may have been accompanied by metasomatic overprinting of the original units. The problem is to distinguish among these several compositional effects and to evaluate each.

Bulk-rock X-ray fluorescence spectroscopy (XRF) major- and minor-element compositions for 55 samples of the Yellow Dog metavolcanic complex (both flows and hypabyssal intrusives) were presented by Ernst (1987, Table 2). Compositional data for an additional 17 greenstone specimens and 2 serpentinites (presented on an anhydrous basis to facilitate comparison with mantle peridotites) are listed in Table 3; also listed are bulk-rock averages for the different Yellow Dog lithologies. Highly magnesian units tentatively classified as komatiitic(?) metabasalts (Ernst, 1987) occur among all three mapped Yellow Dog metavolcanic lithologies (dark green flow breccias, and more massive, lighter-colored lavas + dikes/sills); the Mg-rich rocks are characterized by elevated Cr and Ni contents and by high values of CaO/Al_2O_3.

Rare-earth–element (REE) bulk-rock concentrations were provided by Ernst (1987, Table 3) for 12 Yellow Dog greenstone samples. Instrumental neutron activation analyses for 16 additional meta-igneous rocks are listed in Table 4, along with an average for 16 associated metasediments. Bulk-rock oxygen isotopic proportions were presented by Ernst (1987, Table 5) for six Yellow Dog meta-igneous rocks. $^{18}O/^{16}O$ ratios for 17 additional greenstones, 3 samples of English Peak granodiorite (along with quartz concentrates from two of these samples), and 6 metaclastic rocks are given in Table 5.

Primary Stratigraphic Variations in Bulk-Rock Chemistry

The extrusives and shallow-level intrusives of the Sawyers Bar area exhibit a consistent range

TABLE 4. BULK-ROCK RARE-EARTH-ELEMENT CHEMISTRY OF YELLOW DOG MAFIC META-IGNEOUS ROCKS AND AVERAGE OF 16 ASSOCIATED METASEDIMENTARY ROCKS, SAWYERS BAR TERRANE (ppm)

Rock type	La	Ce	Nd	Sm	Eu	Tb	Yb	Lu
Darker metavolcanic								
91M*	38.7	75	37	7.7	2.90	1.0	1.89	0.24
201M	33.1	63	28	5.4	2.41	1.0	2.00	0.26
372M	15.7	37	19	4.7	1.66	0.5	1.72	0.24
Lighter metavolcanic								
9M*	3.5	9	7	1.9	0.88	0.4	1.94	0.30
85M	3.1	11	6	1.9	0.64	0.4	2.26	0.32
86M	5.2	<1	<3	<0.1	1.20	0.6	2.79	0.41
92M*	0.5	6	<3	0.1	0.17	<0.1	0.19	0.04
127M	3.2	9	6	1.6	0.72	0.3	1.73	0.28
146M	3.1	17	6	2.1	0.56	0.6	2.41	0.35
288M	5.8	19	12	3.3	1.39	0.9	3.91	0.60
391M*	18.6	37	17	3.3	1.28	0.6	1.33	0.18
450M	3.6	10	7	2.1	1.06	0.5	2.23	0.33
516M	3.5	9	7	2.1	1.14	0.5	2.21	0.33
Hypabyssal								
220M	17.5	36	17	4.0	1.12	0.6	2.07	0.27
235M	3.3	15	6	2.2	1.02	0.5	2.23	0.33
285M	16.4	42	19	3.7	1.46	0.7	2.02	0.29
Metasedimentary								
Average of 16	24.0	47.6	22.3	4.76	1.22	0.64	2.34	0.36
Chondrite normalizing value	0.315	0.813	0.597	0.192	0.0722	0.049	0.209	0.0323

*Metakomatiitic(?) basalt.
Neutron activation analyses of Yellow Dog greenstones by X-ray Assay Laboratories, Ltd, Don Mills, Ontario. Neutron activation analyses of metasedimentary rocks by G. W. Kallemeyn, University of California, Los Angeles.

of basaltic compositions and appear to represent two separate magma series. Some of the coarser-grained units described as hypabyssals may instead be slowly cooled flow interiors, but in many cases, poor exposures do not allow this field distinction to be made. Accordingly, massive Yellow Dog metavolcanics retaining original medium- to coarse-grained diabasic textures ± relict, subophitic igneous clinopyroxene and/or prismatic pargasitic hornblende grains are classified as hypabyssals. Intrusive rocks need not adhere to stratigraphic and areal relationships exhibited by the extrusive pile; hence they should not be included where systematic regional contrasts in Yellow Dog protolith bulk-rock chemistry are under consideration. As a practical matter, however, the dikes and sills conform to the compositional and stratigraphic relationships recognized in the lavas, as discussed below.

TABLE 5. BULK-ROCK OXYGEN ISOTOPIC RATIOS FOR YELLOW DOG META-IGNEOUS ROCKS, ASSOCIATED METACLASTICS, AND ENGLISH PEAK PLUTON SAMPLES, SAWYERS BAR AREA

Rock type	Sample no.	$\delta^{18}O$
Darker metavolcanic	91M*	15.89
	170M	13.04
	201M	10.84
	207M	12.10†
	354M*	12.85
	372M	11.32
	386M	10.80
Lighter metavolcanic	46M	13.81
	86M	8.69
	92M*	14.22
	117M	11.15
	146M	9.36
	288M	14.89†
	374M	13.02
	516M	10.58*
Hypabyssal	220M	11.37
	285M	11.46*
Metaclastic	134M	16.63
	166M	14.67
	178M	14.87
	182M	12.36
	197M	17.94
	355M	13.28
English Peak pluton	24M	11.27—quartz = 13.53
	26M	9.0*
	326M	10.4*—quartz = 13.98

*Mg-rich metabasalts
†Average of two analyses

Major-element variation indicates that the darker, more schistose igneous unit, chiefly associated with metasedimentary strata and interpreted as stratigraphically underlying the main mass of Yellow Dog metavolcanics, is compositionally distinct from the paler, more massive, overlying pile of metabasaltics. The dark green metamafics contain relatively high P_2O_5, TiO_2, and $Fe_2O_3^*$, averaging 0.34 ± 0.17, 2.5 ± 0.6, and 13.9 ± 1.2 wt. %, respectively, and are also richer in Hf, Zr, Ta, La, Ce, Nd, Sm, and Eu. The lighter-colored greenstones contain an average of 0.11 ± 0.05, 0.9 ± 0.2, and 10.73 ± 1.0 wt. % P_2O_5, TiO_2, and $Fe_2O_3^*$, respectively. Compared to the main, overlying body of metavolcanics, the darker, mildly alkalic metavolcanic unit contains slightly less MgO and contains less silica, alumina, and soda (Table 3). Among Yellow Dog rock types, the metahypabyssals tend to contain the most SiO_2 and K_2O. None is titaniferous or especially rich in iron; hence, all belong compositionally to the more voluminous light green basalt series (for example, see Fig. 7). With regard to other major and trace elements, the various Yellow Dog greenstone units exhibit comparable bulk-rock chemical variations.

Mg-rich units are widely but sporadically distributed in the Sawyers Bar area. Magnesian metabasalts occur as recrystallized dikes and sills as well as both darker and paler meta-extrusives. No correlation appears to exist between the occurrence of highly magnesian Yellow Dog metavolcanics, their intrusive or extrusive nature, and either inferred stratigraphic position or proximity to later granitoids.

Major + Minor-Element Bulk-Rock Chemistry and Compositional Affinities of the Yellow Dog Melts

Because the studied rocks have been subjected to submarine alteration as well as regional and contact metamorphism, the effects of metasomatism constitute a serious concern. In order to evaluate these subsolidus phenomena, compositional trends must be investigated, and the distinction drawn between igneous and metamorphic processes. Major- and minor-element bulk-chemical variations are plotted for all analyzed Yellow Dog meta-igneous rocks in Figures 7–12. Such diagrams allow determination of the phases controlling bulk-rock compositional variations. Intrusive and extrusive (both Ti + Fe^* + P-rich and Ti + Fe^* + P-poor) protoliths are distinguished. Seventeen of the analyzed rocks (13 extrusives and 4 hypabyssals) are especially Mg rich. Several others (for example, 57M, 86M, and 424M) are transitional in chemical properties between those exhibiting magnesian affinities and the more normal basaltic meta-igneous rocks. Donato (1985) also reported the presence of several metamorphosed dikes, sills, and an amphibole schist characterized by high MgO contents directly north of the northeast corner of the mapped area; the average magnesia content of 8 high-Mg metahypabyssal and metaflow rocks is 13.1 ± 2.4 wt. %, as listed by Donato (1985, tables 1.4, 1.5, and 1.6).

Yellow Dog greenstone bulk-rock analyses are chemographically portrayed in Figure 7 in terms of weight percent TiO_2 versus $Fe^*/(Fe^* + Mg)$. Sample 506M, shown in the illustrations as a darker-colored meta-extrusive, is transitional between titania-rich and titania-poor metavolcanics. Metamorphosed hypabyssal rocks and the paler metalavas display nearly constant, rela-

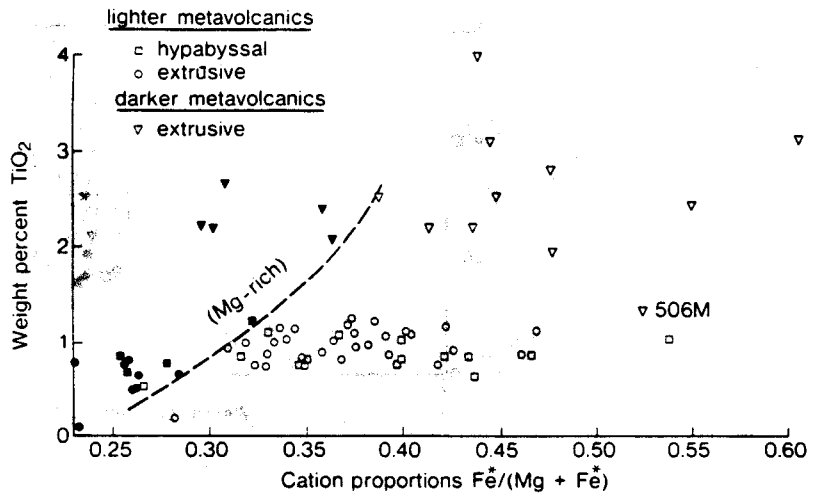

Figure 7. Bulk-rock TiO_2 in weight percent versus molar X_{Fe^*} for Yellow Dog metavolcanics. Sample symbols as in Figure 2. Mg-rich meta-igneous rocks are clearly richer in titanium than are more normal greenstones for a given degree of fractionation (X_{Fe^*}). More importantly, the dark green, schistose flow breccias appear to represent a metamorphosed lava series chemically distinct from the more abundant, paler Yellow Dog metadiabases and metabasalts.

tively low TiO_2 contents, regardless of X_{Fe^*}. Among the extrusives, magnesian metabasalts are slightly more titaniferous than associated greenstones of comparable X_{Fe^*}. Although a range in mole fraction Fe* exists, the komatiitic(?) metabasalts appear to possess lower X_{Fe^*} on the average than do the other meta-extrusives. If the analyzed Mg-rich metavolcanics were olivine ± clinopyroxene–enriched cumulates, the titania contents would be expected to be lower than those of associated parental basalt magmas rather than the same or higher, as is observed. Both darker- and lighter-colored series exhibit this relationship.

The Mg-rich Yellow Dog metavolcanics were previously interpreted tentatively as komatiitic basalts (Ernst, 1987). Such ultramafic lavas are characterized by high CaO/Al_2O_3 weight percent values, as well as by remarkably elevated MgO contents. Viljoen and Viljoen (1969) defined komatiites as having CaO/Al_2O_3 ratios exceeding unity, whereas others (for example, Arndt and Nisbet, 1982; Xu and Chen, 1984) have demonstrated that ratios in the range 0.8–1.0 typify many aphyric komatiitic lavas. Picrites and boninites are also compositionally characterized by abundant magnesia, although most CaO/Al_2O_3 values for such rock types are substantially lower than unity (Crawford, 1989). Bulk-rock ratios of CaO/Al_2O_3 are plotted against MgO in Figure 8 for the Yellow Dog greenstones. The 17 analyzed magnesian samples as a group have distinctive, high (MgO + CaO)/Al_2O_3 proportions. The lack of glomeroporphyritic olivine pseudomorphs even in coarse-grained dike rocks typified by abundant relict igneous phases as well as the probable aphanitic nature of the precursor lavas also are compatible with a parental refractory basalt, rather than a picritic cumulate (Cameron and Nisbet, 1982).

Elevated nickel and chromium contents typify olivine-, chrome diopside–, and chrome spinel–rich rocks. Liquids derived through extensive partial fusion of such precursor crystalline assemblages, therefore, tend to be enriched in

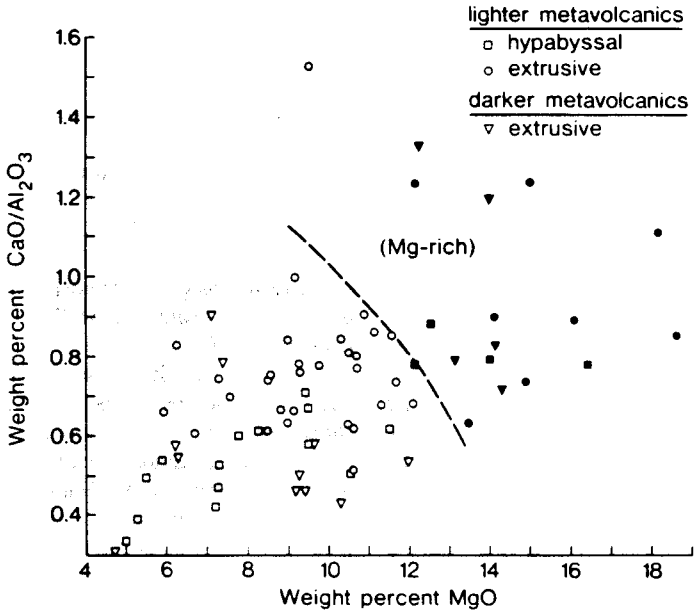

Figure 8. Bulk-rock CaO/Al_2O_3 versus MgO in terms of weight percent for Yellow Dog metavolcanics. Sample symbols as in Figure 2. Magnesian meta-igneous rocks show apparent similarities to komatiitic basalts (and some VAB's).

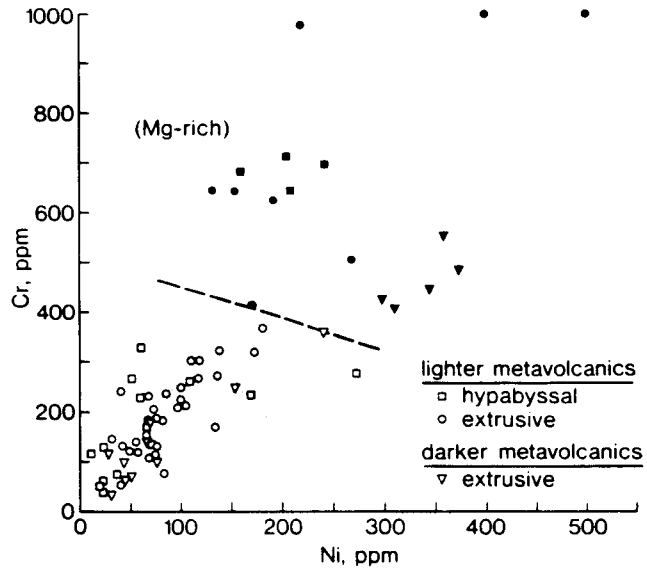

Figure 9. Bulk-rock concentrations of Cr versus Ni in parts per million for Yellow Dog metavolcanics. Sample symbols as in Figure 2. Magnesian meta-igneous rocks show apparent similarities to komatiitic basalts.

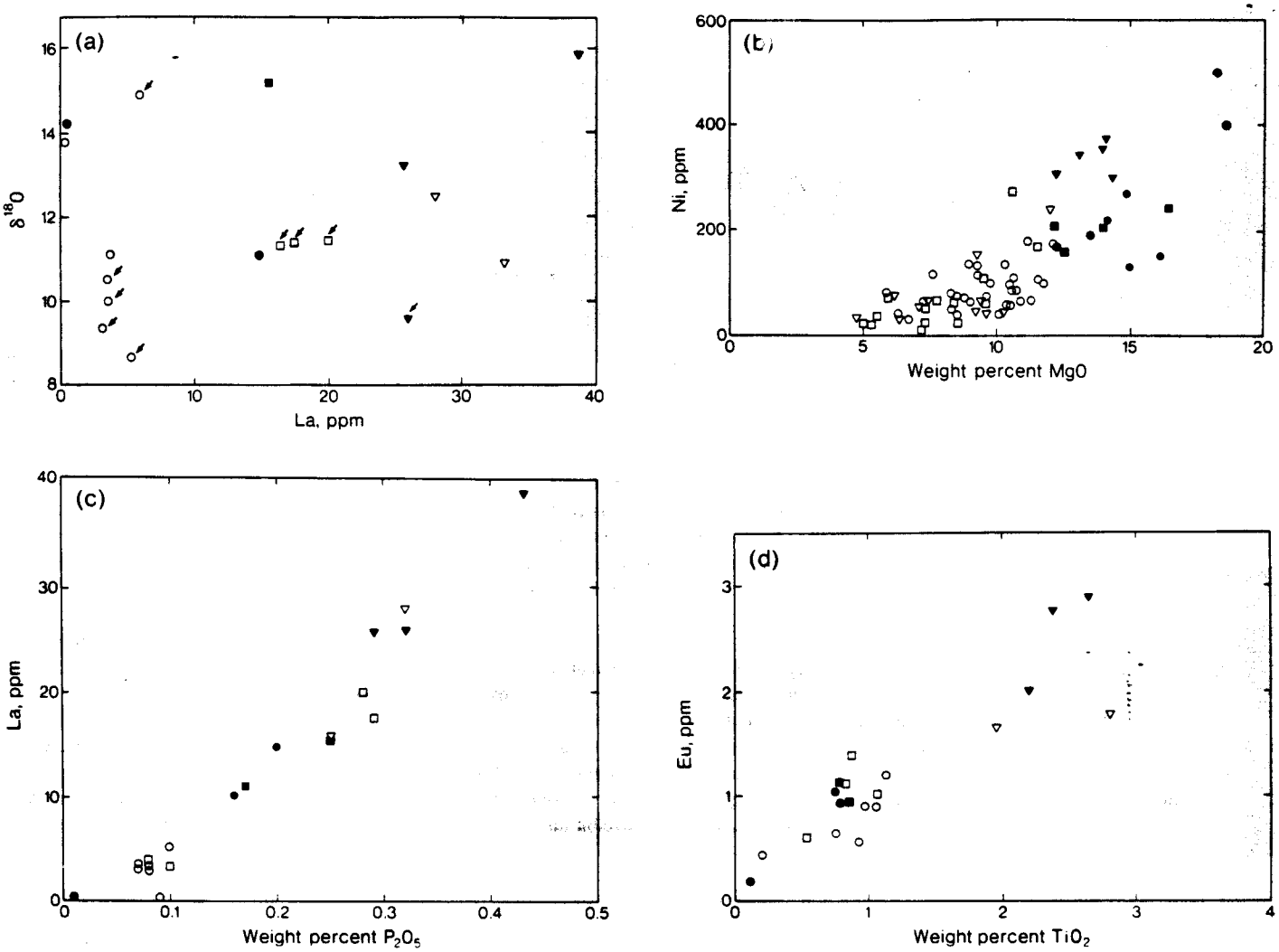

Figure 10. Bulk-rock proportions of various major-element and trace constituents for the Yellow Dog metavolcanics. Sample symbols as in Figure 2. Illustrated systematic trends are characteristic of crystal-melt partitioning. Lack of correlation between $\delta^{18}O$ and La exhibited in part a indicates that metasomatism did not result in covariance of LREE's and oxygen exchange; arrows denote analyzed greenstone samples at least 250 m horizontally removed from the nearest metasedimentary unit.

both elements, whereas olivine-cumulate basalts exhibit high Ni but more nearly normal Cr contents relative to mid-ocean-ridge basalts (MORB's). Oceanic island basalts (OIB's) and immature magmatic arc basalts (IAT's) characteristically are high in both Ni and Cr (Arndt and Nesbitt, 1982). As shown in Figure 9, the Yellow Dog magnesian metabasalts are compositionally distinct, but grade toward the associated metavolcanics of more normal bulk-rock chemistry in terms of Cr and Ni. The darker metalavas tend to possess lower Cr/Ni ratios than do the pabyssals and extrusives.

Additional compositional features of the Yellow Dog metavolcanics, as well as systematic magmatic chemical differentiation trends in minor and trace elements, are portrayed in Figure 10. Oxygen isotopic compositions were strongly modified during regional and contact metamorphism (see below). The absence of a correlation between La and $\delta^{18}O$, and between La concentration and proximity to LREE-rich metasediments, suggest that enrichment of the greenstones in ^{18}O during metamorphism did not systematically involve the REE's (Fig. 10a). The correlation of Ni with MgO and substantial increment in Ni with elevated magnesia contents indicate early-formed crystals concentrated Ni with respect to Mg (Fig. 10b), a characteristic, unambiguously igneous phenomenon. Lanthanum and europium contents vary systematically with P_2O_5 and TiO_2, respectively (Figs. 10c and 10d). Marked bimodality in the chemographic trends is not obvious, although analyses of the darker meta-extrusives tend to form a distinct, high-Ti field. Strong positive correlations also exist between the pair Cr-MgO (similar to Fig. 10b, clearly suggesting the preferential early magmatic removal of Cr, probably in spinel, relative to MgO), between the pairs $Fe_2O_3^*$-TiO_2, P_2O_5-TiO_2, and Zr-P_2O_5, and between the LREE's-Sr, -Zn, -Zr, -TiO_2, and -P_2O_5. Such regular behavior in general is characteristic of igneous processes involving fractional crystallization and/or varying degrees of partial fusion. B. R. Hacker and others (unpub. data), however, have shown that measured major-element abundances were affected by metasomatism; minor- and trace-element concentrations are unlike komatiitic basalts, but compare favorably with alkalic and tholeiitic-arc lavas, as will now be demonstrated.

Spider diagrams for Yellow Dog bulk-rock trace-element data normalized to MORB are presented in Figure 11. With regard to incompatible elements, the darker, ferruginous, titaniferous breccia layers correspond closely to mildly

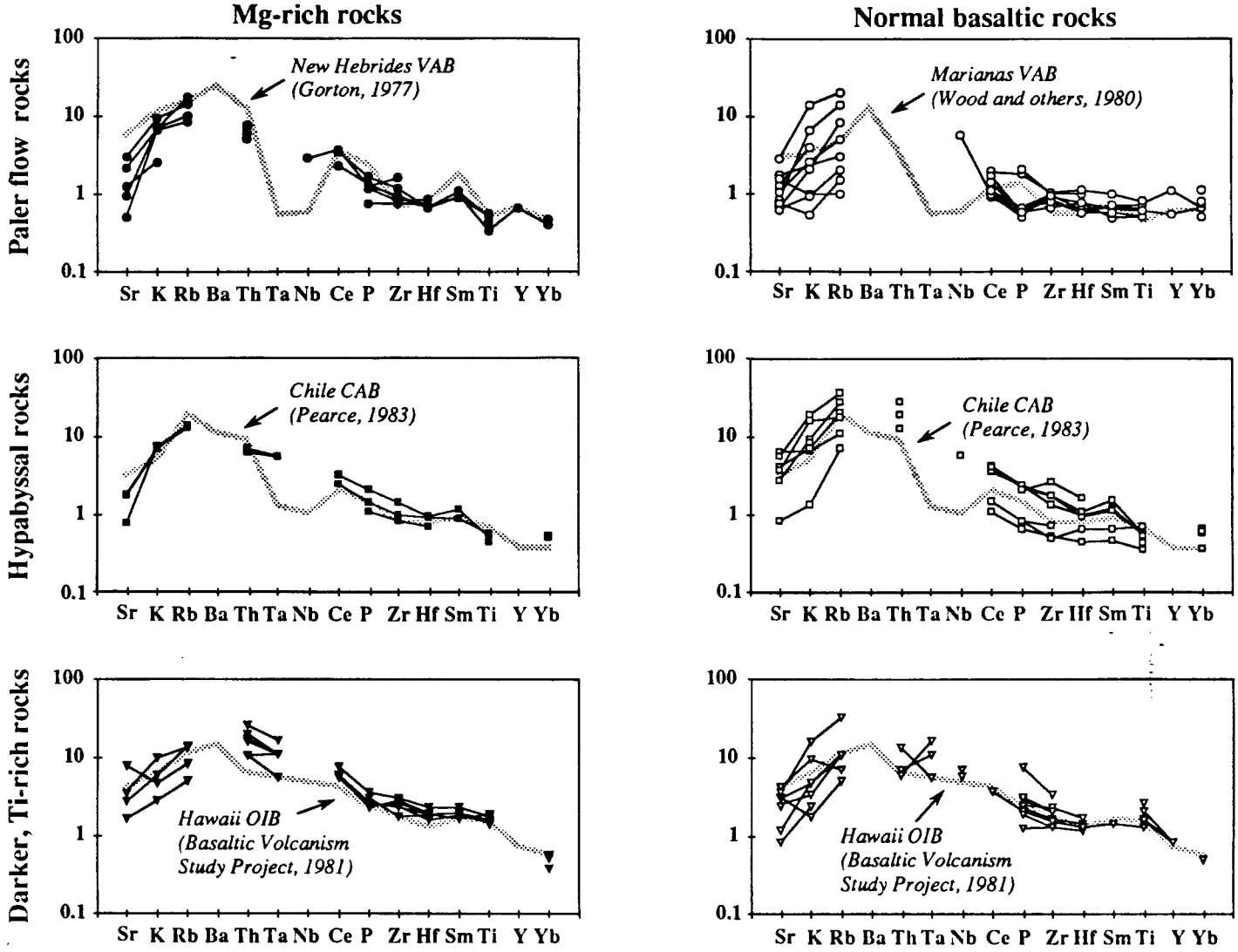

Figure 11. Bulk-rock abundances of incompatible elements in the Yellow Dog volcanics relative to mid-ocean-ridge basalt (MORB) (after Pearce, 1983). Sample symbols as in Figure 2. Heavy gray lines depict MORB-normalized element concentrations of rocks from type tectonomagmatic environments. Paler Yellow Dog metalavas are similar to volcanic arc basalts (IAT's); all have Ta levels below detection (~1 ppm), and many also have less Th than could be detected (~0.5 ppm). Metahypabyssal rocks (Mg-rich and basaltic) are similar but possess more Th and Ta, suggesting derivation from enriched mantle—or fractionation—perhaps in a continental arc setting. Mg-rich meta-extrusives are transitional between these two types. The Ti-rich rocks are distinctly different from the Ti-poor rocks, particularly in their Ti, Hf, and Zr abundances, and are similar to alkalic oceanic island lavas (OIB's).

alkalic OIB's. Such a pattern suggests that the ne-normative characteristics of these greenstones may represent derivation from a suboceanic lithospheric source, rather than being related to postmagmatic alteration. Most of the paler, massive flows and hypabyssals correlate with IAT's and could reflect eruption within an immature magmatic arc. The compositions of analyzed relict igneous hornblendes and clinopyroxenes presented earlier indicate that the bulk compositional spectrum of the darker- and lighter-colored Yellow Dog metavolcanic suites may have been produced by cpx or amphibole fractionation/accumulation, but not by fractionation/accumulation of plagioclase, ilmenite, or olivine. These chemical/mineralogic trends are shown in Figure 12.

In aggregate, the systematic compositional relationships illustrated in Figures 7–12 lead to the following conclusions. (1) Evolved (Fe^* + P + Ti-rich) and nonevolved (Fe^* + P + Ti-poor) members of two distinct melt series are present. (2) Low-Ti basalts and diabases are similar to immature arc basalt (IAT), whereas high-Ti amygdaloidal flow breccias are mildly alkaline (OIB) in character. (3) Igneous differentiation may have been controlled by cpx and/or amphibole fractionation, but not by ilmenite, plagioclase, or olivine. Texturally, Mg-rich bulk-rock compositions do not appear to represent olivine or cpx cumulates. In spite of metasomatism, (4) systematic igneous trends indicate that primary crystal-melt fractionation was also partially responsible for the range of bulk-rock compositions.

Rare-Earth-Element Chemistry

Chondrite-normalized rare-earth patterns for newly and previously analyzed Yellow Dog greenstones are plotted in Figure 13. The dark green flow breccias exhibit consistent LREE en-

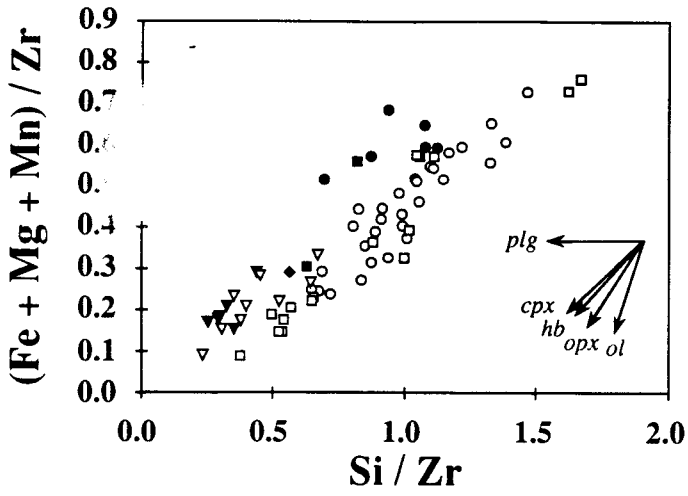

Figure 12. Cation-ratio diagram (Pearce, 1968) demonstrating that compositional variation in the Yellow Dog greenstones may be the result of clinopyroxene or hornblende accumulation or fractionation. The arrows show the (Fe* + Mg + Mn)/Si molar ratios for analyzed bulk rocks and potentially controlling mineral phases (+ hypothetical hypersthene and olivine).

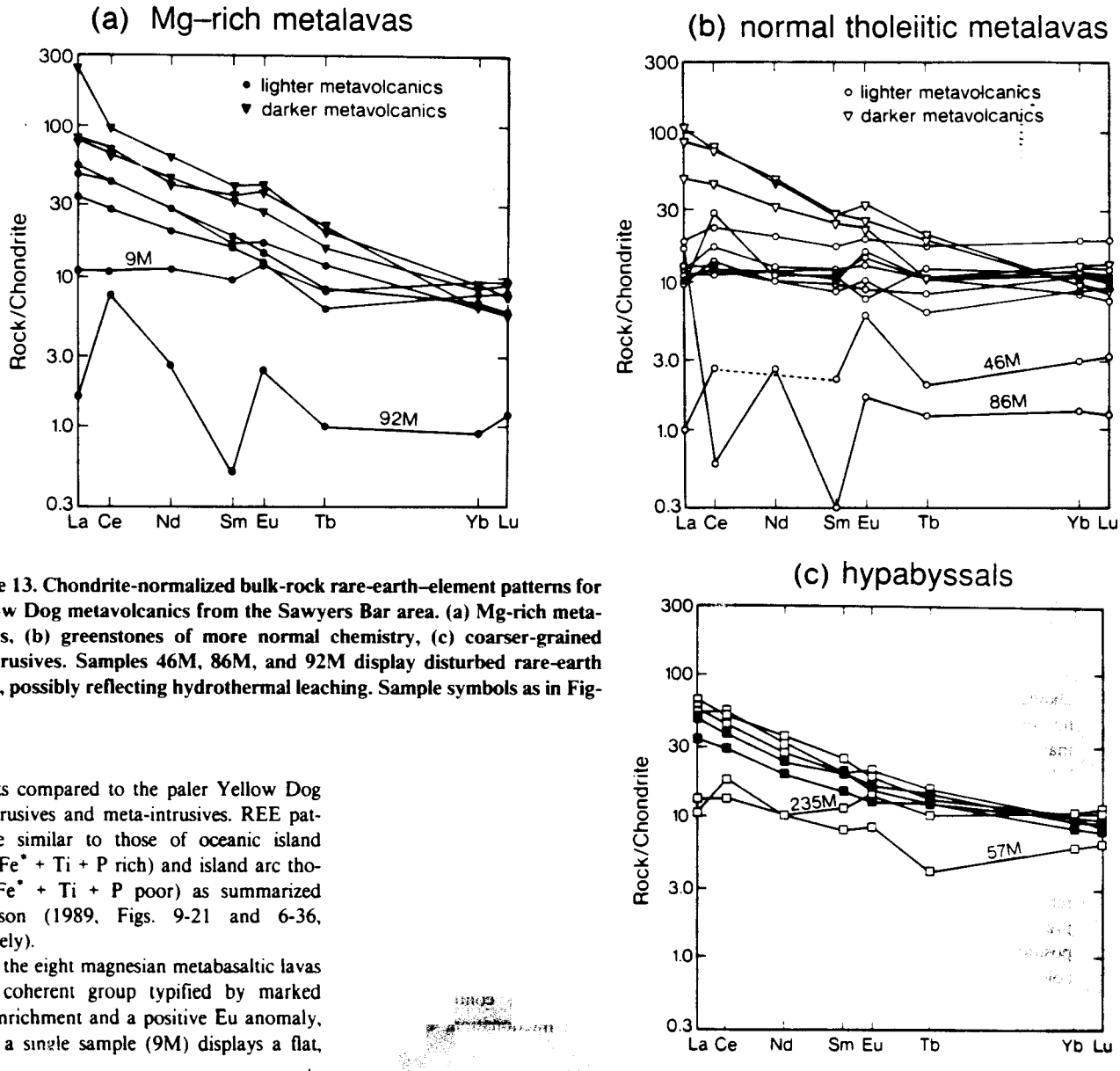

Figure 13. Chondrite-normalized bulk-rock rare-earth–element patterns for 28 Yellow Dog metavolcanics from the Sawyers Bar area. (a) Mg-rich metavolcanics, (b) greenstones of more normal chemistry, (c) coarser-grained meta-intrusives. Samples 46M, 86M, and 92M display disturbed rare-earth patterns, possibly reflecting hydrothermal leaching. Sample symbols as in Figure 2.

richments compared to the paler Yellow Dog meta-extrusives and meta-intrusives. REE patterns are similar to those of oceanic island basalts (Fe* + Ti + P rich) and island arc tholeiites (Fe* + Ti + P poor) as summarized by Wilson (1989, Figs. 9-21 and 6-36, respectively).

Six of the eight magnesian metabasaltic lavas form a coherent group typified by marked LREE enrichment and a positive Eu anomaly, whereas a single sample (9M) displays a flat,

unfractionated pattern. The eighth specimen (92M) exhibits an erratic pattern, with approximately chondritic abundances (Fig. 13a). For these Mg-rich metavolcanics, the three analyzed $Fe^* + P + Ti$-rich metavolcanics are systematically enriched in light rare earths compared to the pale green, Mg-rich metalavas. Among the 13 normal tholeiitic greenstones, three distinct types of pattern may be distinguished (Fig. 13b). The three analyzed $Fe^* + Ti + P$-rich metavolcanics are, like the dark green magnesian basalts, enriched in LREE's compared to the pale metalavas and have positive Eu anomalies. The lighter-colored metavolcanics possess nearly flat patterns. Two of the less magnesian lighter greenstones (46M, 86M) display chondrite-like abundances but disturbed patterns, similar to the Mg-rich metabasalts. These altered REE concentrations may reflect localized metasomatism. Rare-earth-element concentrations for seven samples of coarser-grained, $Fe^* + Ti + P$-poor, Yellow Dog metahypabyssals are presented in Figure 13c. These rocks show moderate LREE enrichment relative to that of chondrites. Two samples, 57M and 235M, exhibit an indistinct tendency toward lower REE abundances and perhaps represent slightly disturbed patterns.

Bulk-Rock Assimilation of North Fork Sedimentary Material by the Yellow Dog Magmas

Contamination of original basaltic liquids by LREE-rich sedimentary units can be ruled out by mass-balance calculations. Patterns for averages of 16 metasediments, 11 REE-unfractionated (parental?) greenstones, and 14 REE-fractionated (contaminated?) greenstones are illustrated in Figure 14. Unacceptably high sediment proportions are required to produce the observed fractionated metavolcanic LREE patterns. For simple mixing, assuming a parental melt characterized by a flat REE pattern, this would require upward of 80%–95% sediment dissolved in the melt to explain the LREE concentrations. Moreover, the product metavolcanic HREE contents are higher than those of either of the putative mixing components. Elevated rare-earth-element contents can be achieved by the combined effects of assimilation and fractional crystallization (AFC); however, even the most favorable AFC model cannot account for REE enrichment in magmas such as the Yellow Dog greenstones that retain an overall metabasaltic bulk composition.

Moreover, major-element contents of the metasedimentary rocks, which are notably richer than the metavolcanics in SiO_2, Al_2O_3, MnO, and alkalis and poorer in total iron, MgO, and TiO_2 (also, in general, in CaO), do not correlate with metavolcanics characterized by fractionated REE patterns. No field, structural, or textural evidence has been found for contamination of the mafic meta-igneous rocks. Finally, as will be presented further on, bulk-rock ϵ_{Nd} values suggest that the metavolcanics have not been substantially modified by crustal contamination.

Oxygen Isotope Variation

Bulk-rock $^{18}O/^{16}O$ analyzes were obtained for 17 Yellow Dog metavolcanic specimens (Table 5). Combined with previously published data for 6 other samples (Ernst, 1987), the 23 analyses allow constraints to be placed on the role of fluids and possible extent of metasomatism during recrystallization of the Yellow Dog melt series. The investigated samples, 7 Mg-rich basalts and 16 of more normal Mg contents, are strongly ^{18}O enriched relative to Phanerozoic MORB's ($\delta^{18}O = +6$; Taylor, 1968; Longstaffe and others, 1977; Hoefs and Binns, 1978; Beaty and Taylor, 1982). At Sawyers Bar, the Mg-rich units overlap isotopically ($\delta^{18}O$ $ave_7 = +13.2 \pm 2.2$) the normal basaltic greenstones and hypabyssals ($\delta^{18}O$ $ave_{16} = +11.5 \pm 1.6$). Clearly, all analyzed metabasaltic rocks have exchanged isotopically with large quantities of fluid under low-grade metamorphic conditions. No systematic isotopic contrast exists between darker- and lighter-colored metaflows, or between extrusives versus dikes and sills. Such high-$\delta^{18}O$ mafic rocks characterize many ophiolites where low-temperature exchange with sea water has resulted in bulk-rock $\delta^{18}O$ values in the range +10 to +15 (Gregory and Taylor, 1981; Elthon and others, 1984; Muehlenbachs, 1986; Hoffman and others, 1986).

Correlations between $\delta^{18}O$ enrichment and chromium, nickel, or magnesium contents are not evident in the greenstones of Sawyers Bar, nor are the REE, SiO_2, Na_2O, or K_2O contents, or modes of minerals such as alkali feldspars and/or micas, related to $\delta^{18}O$—as might be expected if regional and/or contact metasomatism had modified bulk-rock concentrations in these units. Therefore, although the Yellow Dog metavolcanics have been subjected to the throughput of large volumes of an ^{18}O-enriched fluid during one or more recrystallization events, most major-, trace-, and rare-earth-element compositions of these greenstones probably were not substantially modified by the process that generated the marked ^{18}O enrichment.

Areal Metamorphic Variations in Bulk-Rock REE and $\delta^{18}O$ Chemistry

Some Yellow Dog units have flat, unfractionated REE patterns at about three times chondritic abundances. Others are strongly fractionated and light-rare-earth-element enriched, whereas three of the analyzed metabasalts are clearly disturbed (Fig. 13). The origin of the strongly modified bulk-rock REE patterns is not well understood. Two of these meta-extrusives (46M, 92M) are intimately interlayered with volumetrically predominant metasedimentary strata adjacent to the English Peak stock; in contrast, the third analyzed greenstone characterized by disturbed REE abundances is a pale Yellow Dog metalava (86M) located well within the main pile of massive flows, far from any metaclastic units and/or granitoid body. The lower

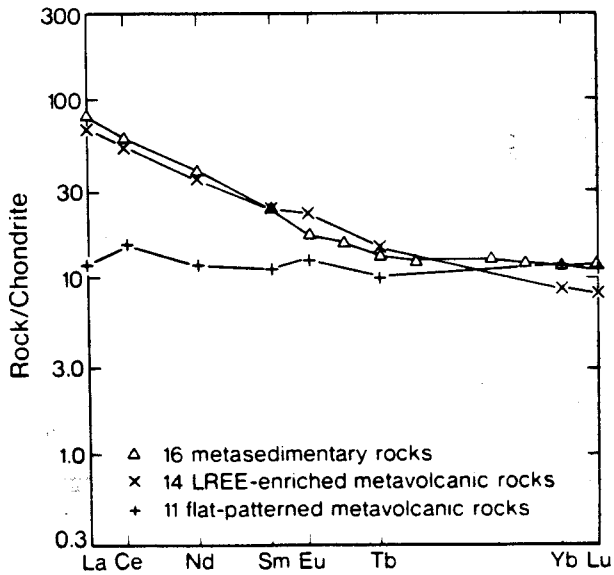

Figure 14. Average bulk-rock chondrite-normalized rare-earth-element patterns for nonevolved (pluses) and fractionated (crosses) Yellow Dog metavolcanics, and for associated metasediments (open triangles), from the Sawyers Bar area. Because of the averaging scheme, sample symbols do *not* conform to usage in the other figures.

concentrations of rare earths combined with generally high $^{18}O/^{16}O$ values (Table 5) are consistent with hydrothermal leaching of these altered rocks.

In general, metavolcanic samples associated with metasedimentary strata and located near the English Peak and Russian Peak plutons tend to be REE fractionated and LREE enriched; these preferentially include the dark green Ti + Fe^* + P-rich greenstones. In contrast, greenstones characterized by more nearly flat REE patterns (mostly the lighter, stratigraphically higher units) are spatially removed from the plutons and/or are not characteristically interlayered with metasedimentary strata. Conceivably, heating accompanying emplacement of the English Peak + Russian Peak granitoids mobilized REE-bearing fluids derived from the metasediments, nearly all of which are strongly LREE enriched, locally metasomatizing and imparting an elevated LREE signature to the metavolcanic suite; however, this seems unlikely, given other elemental trends previously described and lack of correlation of LREE's with proximity to the plutons (Fig. 15a).

In contrast to the REE contents, oxygen isotope compositions of the greenstones vary systematically with respect to distance from granitoid contacts and spatially associated metasedimentary units. Thirteen analyzed greenstones close to metasediments have especially high $\delta^{18}O$ values, with bulk-rock $\delta^{18}O$ averaging +12.9 ± 1.6. Nine other samples, more distant from these strata, possess slightly lower $\delta^{18}O$, averaging +10.8 ± 1.8. One of two Yellow Dog rocks adjacent to the English Peak body, but not interlayered with metasediments (288M), is enriched in ^{18}O, whereas a second (285M) possesses a much lower bulk-rock value. Variability illustrated in Figure 15b may reflect heterogeneous, somewhat channelized fluid flow. Regardless of the degree of proximity of the metasedimentary units, however, $\delta^{18}O$ values in the metavolcanics increase markedly toward the plutons.

If one judges from the limited data presented in Table 5, the English Peak and Russian Peak intrusions themselves are too poor in ^{18}O ($\delta^{18}O$ for three granodioritic specimens averages +10.2 ± 1.2) to have constituted the source of heavy oxygen during high-temperature contact metamorphism; in contrast, the metaclastic strata appear to be relatively heavy ($\delta^{18}O$ bulk-rock values range between +12.36 and +17.94 with an average for the 6 analyzed samples of +15.0 ± 2.1). Evidently, large volumes of recirculating fluids were thermally mobilized from the adjacent metasedimentary section during contact metamorphism accompanying intrusion of the English Peak and Russian Peak magmas; these strata thus provided the main reservoir for ^{18}O exchange with the Yellow Dog metavolcanics.

ϵ_{Nd} Values for Yellow Dog Greenstones

Mafic rocks belonging to the North Fork ophiolite lie directly south along strike of the metavolcanic complex in the Sawyers Bar area, hence probably represent its southern extension. On the basis of the discordant U/Pb age reported by Ando and others (1983) for a metagabbro sample, for the purpose of computation we assume a Permian-Triassic time of formation (~265 Ma) for both North Fork ophiolite and Yellow Dog meta-igneous lithologies. The Yellow Dog greenstones might be considerably younger, however, judging by late-stage, petrographically similar dikes that transect the associated lower Mesozoic sedimentary units (some as young as Early Jurassic) as well as the Stuart Fork complex.

Isotopic Nd and Sm data were obtained for three Yellow Dog samples at the University of California, Los Angeles, by Rosemary Capo. Nominal bulk-rock ϵ_{Nd} values at the assumed ~265 Ma time of ophiolitic melt generation and eruption for the different rock types are darker metavolcanic (11M), +4.8; lighter metaflow (215M), +7.9; metahypabyssal (351M), +3.2. $^{87}Sr/^{86}Sr$ ratios for these specimens at the time of generation were 0.7037, 0.7032, and 0.7055, respectively. Such values are appropriate for somewhat depleted mantle protoliths and suggest that the greenstones exposed near Sawyers Bar are immature IAT- or OIB-like and have been little modified by contamination involving old continental crust.

GEOCHEMICAL/TECTONIC INTERPRETATION OF THE SAWYERS BAR TERRANE

The intimate interlayering with distal turbidites and the interpretation that the extrusive section largely overlies the sediments argue for construction in a continental rise/island arc setting. Metadiabase dikes and sills in the metasedimentary section also attest to roughly coeval deposition and eruption. As shown by the geochemical studies, the predominantly basaltic volcanics include somewhat more evolved arc tholeiites laid down over mildly alkalic, intraplate, oceanic island basalts. These relations support the hypothesis of formation in an immature magmatic arc sited on oceanic crust.

Together, the tectonomagmatic trace- and minor-element discriminant diagrams of Mes-

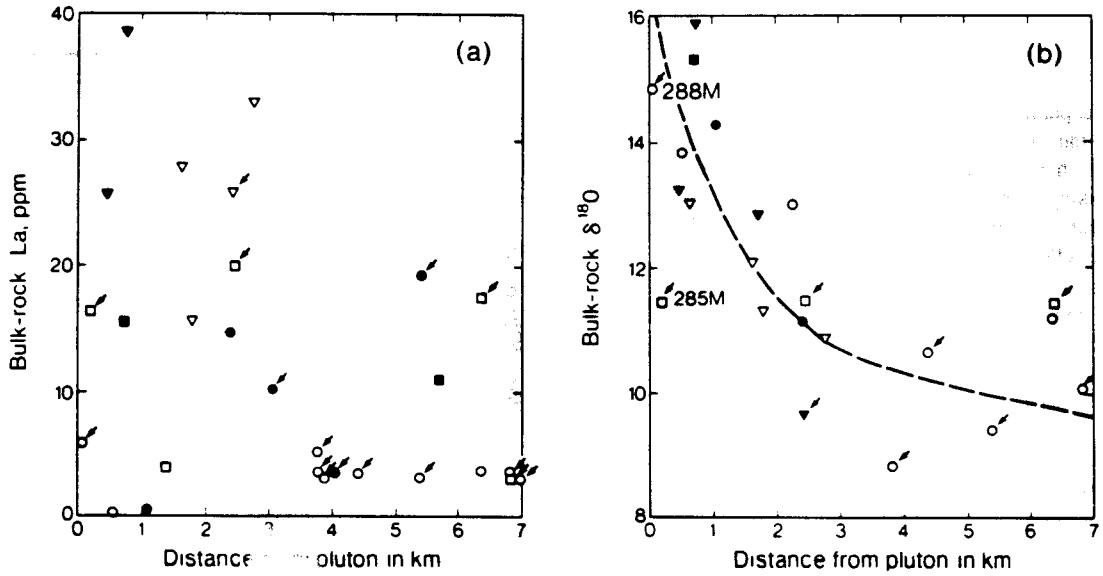

Figure 15. Relationship between proximity of Yellow Dog metavolcanics to Middle/Late Jurassic granitoids in the Sawyers Bar area and (a) bulk-rock La concentration in greenstones and (b) bulk-rock $\delta^{18}O$ values in greenstones. Sample symbols as in Figure 2. Arrows indicate analyzed greenstone samples sited at least 250 m horizontally from the nearest metasedimentary unit. Localities 285M and 288M are close to the English Peak intrusion, but far from metasedimentary units.

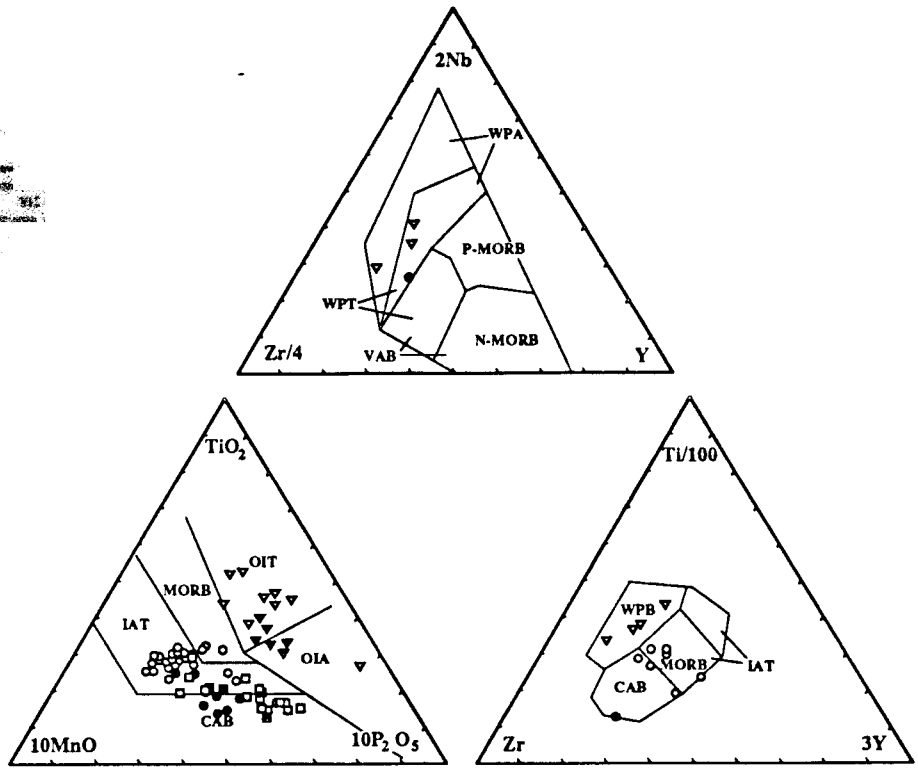

Figure 16. Bulk-rock Nb-Zr-Y, TiO_2-MnO-P_2O_5, and Ti-Zr-Y tectonomagmatic discrimination diagrams of Meschede (1986), Mullen (1983), and Pearce and Cann (1973). Element proportions indicate that the Fe* + P + Ti-rich amygdaloidal flow breccias are probably within-plate basalts, whereas the lighter-colored, more massive samples are immature island-arc tholeiites. Sample symbols as in Figure 2. WPB, within-plate basalt; CAB, continental-arc basalt; IAT, island-arc tholeiite; VAB, oceanic-arc basalt; MORB, mid-ocean-ridge basalt.

chede (1986), Mullen (1983), and Pearce and Cann (1973) indicate that the darker, schistose Fe* + P + Ti-rich flow breccias apparently are within-plate oceanic basalts, and the more massive, pale greenstones are immature island-arc basalts, as illustrated in Figure 16. The former exhibit mildly alkalic tendencies; the latter show mixed arc-tholeiite affinities. Inferences for the origin of the Yellow Dog greenstones are supported by the spidergrams (Fig. 11) and REE abundances (Fig. 13).

Th/Yb and Ta/Yb ratios in arc rocks can be employed to separate subduction-related components from mantle components (Pearce, 1982). Yb is used as the denominator to attempt to eliminate variations in composition caused by partial melting and fractional crystallization. Th and Ta are enriched equally during mantle melting, so that compositions of mid-ocean-ridge and within-plate basalts form a band with a slope of one. Compositional fields are shown in Figure 17. Th enrichment in the source, probably by a slab-derived fluid component during subduction, displaces oceanic island-arc and continental-margin lavas to higher thorium values. Figure 17 indicates that most analyzed hypabyssal samples were produced by partial melting above a subduction zone, whereas Fe* + P + Ti-rich flow breccias were derived from a more enriched mantle source and share affinities with intraplate oceanic basalts. Concentrations of Th and Ta are below detection limits in the paler meta-extrusives, so that their ratios to Yb cannot be portrayed in Figure 17.

The Ti-poor flows and hypabyssal rocks cannot be differentiated from each other based on immobile-trace-element concentrations, but the darker lavas are distinctly different from the overlying lighter-colored suite, particularly in their Ti, Hf, and Zr abundances (see Fig. 12 and other chemographic relations evident from Figs. 7, 10, 11, 11c, 11d, 13a, 13b, and 16). Boninites (Hickey and Frey, 1982), immature island-arc rocks, depleted back-arc-basin basalts, and oceanic tholeiites are not similar in composition to the darker Yellow Dog greenstones, principally because the former groups are not so rich in Ta and Nb.

In summary, the dark, Ti-rich lavas are interpreted provisionally as mildly alkalic, intraplate ocean-island basalts, and the pale, Ti-poor greenstones as immature island arc tholeiites. This is compatible with geologic-structural-stratigraphic relationships in the Sawyers Bar area. The dark green metavolcanics formed early during deposition of the continental-rise terrigenous section in an apparently oceanic, within-plate setting, followed by later extrusion and intrusion of paler, more massive eruptives, as an "outboard" oceanic crust-capped lithospheric plate apparently descended beneath the evolving Sawyers Bar immature island arc. Collapse of a hypothesized "inboard" marginal basin resulted

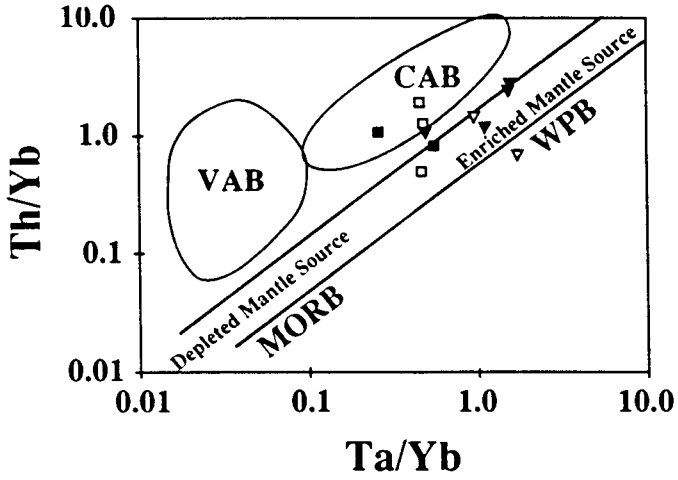

Figure 17. Bulk-rock Th/Yb versus Ta/Yb diagram, illustrating that the dark, Fe* + P + Ti-rich Yellow Dog flow breccias were produced by melting of enriched mantle, probably in a mid-plate setting, whereas the paler hypabyssal units were generated in an island-arc environment. Sample symbols as in Figure 2. WPB, within-plate basalt; CAB, continental-arc basalt; VAB; oceanic-arc basalt; MORB, mid-ocean-ridge basalt.

in collisional encounter of the evolving Sawyers Bar terrane on the west with the previously accreted Stuart Fork subduction complex on the east and thrusting of the latter over the former.

ACKNOWLEDGMENTS

This research was undertaken at the University of California, Los Angeles, supported in early stages by the U.S. Geological Survey and more recently by the Department of Energy through Grant DE FG03-87ER13806. Technical help was provided by Rosemary Capo, R. E. Jones, Ram Alkaly, G. Stummer, G. Kallemeyn, and D. Winter. The manuscript, written and revised at Stanford, was reviewed and improved by C. G. Barnes, J. S. Beard, R. G. Coleman, D. Elthon, and F. A. Frey. The authors are much indebted to the above-named institutions and researchers for help.

REFERENCES CITED

Ando, C. J., Irwin, W. P., Jones, D. L., and Saleeby, J. B., 1983, The ophiolitic North Fork terrane in the Salmon River region, central Klamath Mountains, California: Geological Society of America Bulletin, v. 94, p. 236–252.

Apted, M. J., and Liou, J. G., 1983, Phase relations among greenschist, epidote amphibolite and amphibolite in a basaltic system: American Journal of Science, v. 283A, p. 328–354.

Arndt, N. T., and Nesbitt, R. W., 1982, Geochemistry of Munro Township basalts, *in* Arndt, N. T., and Nisbet, E. G., eds., Komatiites: London, United Kingdom, George Allen and Unwin, p. 309–329.

Arndt, N. T., and Nisbet, E. G., 1982, What is a komatiite?, *in* Arndt, N. T., and Nisbet, E. G., eds., Komatiites: London, United Kingdom, George Allen and Unwin, p. 19–28.

Basaltic Volcanism Study Project, 1981, Basaltic volcanism on the terrestrial planets: New York, Pergamon Press, 1,286 p.

Beaty, D. W., and Taylor, H. P., Jr., 1982, The oxygen isotope geochemistry of komatiites: Evidence for water-rock interaction, *in* Arndt, N. T., and Nisbet, E. G., eds., Komatiites: London, United Kingdom, George Allen and Unwin, p. 267–280.

Blake, M. C., Jr., Howell, D. G., and Jones, D. L., 1982, Preliminary tectonostratigraphic terranes map of California: U.S. Geological Survey Open-File Report 82-593.

Borns, D. J., 1984, Eclogites in the Stuart Fork terrane, Klamath Mountains, California: Geological Society of America Abstracts with Programs, v. 16, p. 271.

Burchfiel, B. C., and Davis, G. A., 1981, Triassic and Jurassic tectonic evolution of the Klamath Mountains-Sierra Nevada geologic terrane, *in* Ernst, W. G., ed., The geotectonic development of California: Englewood Cliffs, New Jersey, Prentice-Hall, p. 50–70.

Cameron, W. E., and Nisbet, E. G., 1982, Phanerozoic analogues of komatiitic basalts, *in* Arndt, N. T., and Nisbet, E. G., eds., Komatiites: London, United Kingdom, George Allen and Unwin, p. 29–49.

Coleman, R. G., Mortimer, N., Donato, M. M., Manning, C. E., and Hill, L. B., 1988, Tectonic and regional metamorphic framework of the Klamath Mountains and adjacent Coast Ranges, California and Oregon, *in* Ernst, W. G., ed., Metamorphism and crustal evolution of the western United States: Englewood Cliffs, New Jersey, Prentice-Hall, p. 1061–1097.

Cotkin, S. J., and Armstrong, R. L., 1987, Rb/Sr age, geochemistry, and tectonic significance of blueschist from the schist of Skookum Gulch, eastern Klamath Mountains, California: Introducing the Callahan event: Geological Society of America Abstracts with Programs, v. 19, p. 367–368.

Crawford, A. J., ed., 1989, Boninites: London, United Kingdom, Unwin Hyman, 465 p.

Davis, G. A., 1968, Westward thrusting in the south-central Klamath Mountains, California: Geological Society of America Bulletin, v. 79, p. 911–933.

Donato, M. M., 1985, Metamorphic and structural evolution of an ophiolitic tectonic melange, Marble Mountains, northern California [Ph.D. dissert.]: Stanford, California, Stanford University, 258 p.

——1987, Evolution of an ophiolitic tectonic melange, Marble Mountains, northern California Klamath Mountains: Geological Society of America Bulletin, v. 98, p. 448–464.

——1989, Metamorphism of an ophiolitic tectonic melange, northern California Klamath Mountains, USA: Journal of Metamorphic Geology, v. 7, p. 515–528.

Donato, M. M., Barnes, C. G., Coleman, R. G., Ernst, W. G., and Kays, M. A., 1982, Geologic map of the Marble Mountain Wilderness, Siskiyou County, California: U.S. Geological Survey Map MF-1452A, scale 1:48,000.

Elthon, D., Lawrence, J. R., Hanson, R. E., and Stern, C., 1984, Modelling of oxygen isotope data from the Sarmiento ophiolite complex, Chile, *in* Gass, I. G., Lippard, S. J., and Shelton, A. W., eds., Ophiolites and oceanic lithosphere: Geological Society of London Publication No. 13, p. 185–197.

Ernst, W. G., 1987, Mafic meta-igneous arc rocks of apparent komatiitic affinities, Sawyers Bar area, central Klamath Mountains, northern California, *in* Mysen, B. O., ed., Magmatic processes: Physico-chemical principles: Geochemical Society Special Publication No. 1, p. 191–208.

——1991, Accretionary terrane in the Sawyers Bar area of the western Triassic and Paleozoic belt, central Klamath Mountains, northern California: Geological Society of America Special Paper (in press).

Goodge, J. W., 1989a, Polyphase metamorphism of the Stuart Fork terrane, a Late Triassic subduction complex, Klamath Mountains, northern California: American Journal of Science, v. 289, p. 874–943.

——1989b, Early to middle Mesozoic deformation of a convergent margin complex, Klamath Mountains, northern California: Tectonics, v. 8, p. 845–864.

Gorton, M. P., 1977, The geochemistry and origin of Quaternary vulcanism in the New Hebrides: Geochimica et Cosmochimica Acta, v. 41, p. 1257–1270.

Gregory, R. T., and Taylor, H. P., 1981, An oxygen isotope profile in a section of Cretaceous oceanic crust, Samail Ophiolite, Oman: Evidence for $\delta^{18}O$ buffering of the oceans by deep (<5 km) seawater-hydrothermal circulation at mid-oceanic ridges: Journal of Geophysical Research, v. 86, p. 2737–2755.

Hickey, R. L., and Frey, F. A., 1982, Geochemical characteristics of boninite series volcanics: Implications for their source: Geochimica et Cosmochimica Acta, v. 46, p. 2099–2115.

Hill, L. B., 1985, Metamorphic, deformational, and temporal constraints on terrane assembly, northern Klamath Mountain, California, *in* Howell, D. G., ed., Tectonostratigraphic terranes of the circum-Pacific region: Houston, Texas, Circum-Pacific Council on Energy and Mineral Resources, No. 1, p. 173–186.

Hoefs, J., and Binns, R. A., 1978, Oxygen isotope compositions in Archean rocks from Western Australia, with special reference to komatiites: U.S. Geological Survey Open-File Report 78-701, p. 180–182.

Hoffman, S. E., Wilkon, M., and Stakes, D. S., 1986, Inferred oxygen isotope profile of Archean oceanic crust, Onverwacht Group, South Africa: Nature, v. 321, p. 55–58.

Hotz, P. E., 1973, Blueschist metamorphism in the Yreka-Fort Jones area, Klamath Mountains, California: U.S. Geological Survey Journal of Research, v. 1, p. 53–61.

Hotz, P. E., Lanphere, M. A., and Swanson, D. A., 1977, Triassic blueschists from northern California and north-central Oregon: Geology, v. 5, p. 659–663.

Irwin, W. P., 1960, Geologic reconnaissance of the northern Coast Ranges and the southern Klamath Mountains, California, with a summary of the mineral resources: California Division of Mines Bulletin, v. 179, 80 p.

——1972, Terranes of the western Paleozoic and Triassic belt in the southern Klamath Mountains, California: U.S. Geological Survey Professional Paper, v. 800-C, p. 103–111.

——1981, Tectonic accretion of the Klamath Mountains, *in* Ernst, W. G., ed., The geotectonic development of California: Englewood Cliffs, New Jersey, Prentice-Hall, p. 29–49.

——1985, Age and tectonics of plutonic belts in accreted terranes of the Klamath Mountains, California and Oregon, *in* Howell, D. G., ed., Tectonostratigraphic terranes of the circum-Pacific region: Houston, Texas, Circum-Pacific Council on Energy and Mineral Resources, Earth Science Series No. 1, p. 187–199.

Irwin, W. P., Jones, D. L., and Kaplan, T. A., 1978, Radiolarians from pre-Nevadan rocks of the Klamath Mountains, California and Oregon, *in* Howell, D. G., and McDougall, K. A., eds., Mesozoic paleography of the western United States: Society of Economic Paleontologists and Mineralogists, Pacific Section, Los Angeles, California, p. 303–310.

Laird, J., and Albee, A. L., 1981, Pressure, temperature, and time indicators in mafic schist: Their application to reconstructing the polymetamorphic history of Vermont: American Journal of Science, v. 281, p. 127–175.

Lanphere, M. A., Irwin, W. P., and Hotz, P. E., 1968, Isotopic age of the Nevadan orogeny and older plutonic and metamorphic events in the Klamath Mountains, California: Geological Society of America Bulletin, v. 79, p. 1027–1052.

Leake, B. E., 1978, Nomenclature of amphiboles: Canadian Mineralogist, v. 16, p. 501–520.

Liou, J. G., Kuniyoshi, S., and Ito, K., 1974, Experimental studies of the phase relations between greenschist and amphibolite in a basaltic system: American Journal of Science, v. 274, p. 613–632.

Longstaffe, F. J., McNutt, R. J., and Schwartz, H. P., 1977, Geochemistry of Archean rocks from the Lake Despair area, Ontario: A preliminary report: Geological Survey of Canada Paper, v. 77-1A, p. 169–178.

Mankinen, E. A., Irwin, W. P., and Gromme, C. S., 1989, Paleomagnetic study of the eastern Klamath terrane, California, and implications for the tectonic history of the Klamath Mountains province: Journal of Geophysical Research, v. 94, p. 10444–10472.

Meschede, M., 1986, A method of discriminating between different types of mid-ocean ridge basalts and continental tholeiites with the Nb-Zr-Y diagram: Chemical Geology, v. 56, p. 207–218.

Mortimer, N., 1985, Structural and metamorphic aspects of Middle Jurassic terrane juxtaposition, northeastern Klamath Mountains, California, *in* Howell, D. G., ed., Tectonostratigraphic terranes of the circum-Pacific region: Houston, Texas, Circum-Pacific Council on Energy and Mineral Resources, Earth Science Series No. 1, p. 201–214.

Muehlenbachs, K., 1986, Alteration of the oceanic crust and the ^{18}O history of seawater, *in* Valley, J. W., Taylor, H. P., Jr., and O'Neil, J. R., eds., Stable isotopes in high temperature geologic processes: Reviews in Mineralogy, v. 16, p. 425–444.

Mullen, E. D., 1983, $MnO/TiO_2/P_2O_5$: A minor element discriminant for basaltic rocks of oceanic environments and its implications for petrogenesis: Earth and Planetary Science Letters, v. 62, p. 53–62.

Nisbet, E. G., and Pearce, J. A., 1977, Clinopyroxene composition in mafic lavas from different tectonic settings: Contributions to Mineralogy and Petrology, v. 63, p. 149–160.

Pearce, J. A., 1982, Trace element characteristics of lavas from destructive plate boundaries, *in* Thorpe, R., ed., Andesites: Orogenic andesites and related rocks: Chichester, United Kingdom, Wiley, p. 525–548.

——1983, The role of sub-continental lithosphere in magma genesis at destructive plate margins, *in* Hawkesworth, C. J., and Norry, M. J., eds., Continental basalts and mantle xenoliths: Nantwich, United Kingdom, Shiva, p. 230–249.

Pearce, J. A., and Cann, J. R., 1973, Tectonic setting of basic volcanic rocks determined using trace element analyses: Earth and Planetary Science Letters, v. 19, p. 290–300.

Pearce, T. H., 1968, A contribution to the theory of variation diagrams: Contributions to Mineralogy and Petrology, v. 19, p. 142–157.

Saunders, A. D., and Tarney, J., 1979, The geochemistry of basalts from a back-arc spreading centre in the East Scotia Sea: Geochimica et Cosmochimica Acta, v. 43, p. 555–572.

Silberling, N. J., Jones, D. L., Blake, M. C., Jr., and Howell, D. G., 1987, Lithotectonic terrane map of the western conterminous United States: U.S. Geological Survey Miscellaneous Field Studies Map MF-1874-C, scale 1:2,500,000.

Snoke, A. W., Sharp, W. D., Wright, J. B., and Saleeby, J. B., 1982, Significance of mid-Mesozoic peridotitic to dioritic intrusive complexes, Klamath Mountains—Western Sierra Nevada, California: Geology, v. 10, p. 160–166.

Taylor, H. P., Jr., 1968, The ^{18}O geochemistry of igneous rocks: Contributions to Mineralogy and Petrology, v. 19, p. 1–71.

Viljoen, M. J., and Viljoen, R. P., 1969, Evidence for the existence of a mobile extrusive peridotitic magma from the Komati formation of the Onverwacht group: Geological Society of South Africa Special Publication 2, Upper Mantle Project, p. 87–112.

Viljoen, M. J., Viljoen, R. P., and Pearton, T. N., 1982, The nature and distribution of Archaean komatiite volcanics in South Africa, *in* Arndt, N. T., and Nisbet, E. G., eds., Komatiites: London, United Kingdom, Allen and Unwin, p. 53–80.

Wagner, P. L., and Saucedo, G. L., 1987, Geologic map of the Weed quadrangle: California Division of Mines and Geology, scale 1:250,000.

Wilson, M., 1989, Igneous petrogenesis: London, United Kingdom, Unwin Hyman, 466 p.

Wood, D. A., Joron, J. L., Marsh, N. G., Tarney, J., and Treuil, M., 1980, Major- and trace-element variations in basalts from the North Philippine Sea drilled during DSDP Leg 58: A comparative study of back-arc-basin basalts with lava series from Japan and mid-ocean ridges, *in* Initial reports of the Deep Sea Drilling Project (Volume 58): Deep Sea Drilling Project, p. 873–894.

Wright, J. E., 1982, Permo-Triassic accretionary subduction complex, southwestern Klamath Mountains, northern California: Journal of Geophysical Research, v. 87, p. 3805–3818.

Wright, J. E., and Fahan, M. R., 1988, An expanded view of Jurassic orogenesis in the western United States Cordillera: Middle Jurassic (pre-Nevadan) regional metamorphism and thrust faulting within an active arc environment, Klamath Mountains, California: Geological Society of America Bulletin, v. 100, p. 859–876.

Xu, G. R., and Chen, H. J., 1984, A preliminary study of komatiites in Anshan-Benxi-Fushun region, northeast China: Geochemistry, v. 8, p. 128–141.

MANUSCRIPT RECEIVED BY THE SOCIETY JANUARY 16, 1990
REVISED MANUSCRIPT RECEIVED MAY 11, 1990
MANUSCRIPT ACCEPTED MAY 23, 1990